

(U)

SECURITY CLASSIFICATION OF THIS PAGE

REPORT DOCUMENTATION PAGE

Form Approved
OMB No. 0704-0188

AD-A211 612

ELECTE

AUG 10 1989

SCHEDULE

1b RESTRICTIVE MARKINGS

NA

3. DISTRIBUTION / AVAILABILITY OF REPORT

Distribution Unlimited

4. PERFORMING ORGANIZATION REPORT NUMBER(S)

89-036

5. MONITORING ORGANIZATION REPORT NUMBER(S)

NA

6a. NAME OF PERFORMING ORGANIZATION

University of Utah

6b. OFFICE SYMBOL
(If applicable)

NA

7a. NAME OF MONITORING ORGANIZATION

Office of Naval Research

6c. ADDRESS (City, State, and ZIP Code)

Salt Lake City, Utah 84112

7b. ADDRESS (City, State, and ZIP Code)

800 N. Quincy Street
Arlington, Virginia 22217-50008a. NAME OF FUNDING / SPONSORING
ORGANIZATION

Office of Naval Research

8b. OFFICE SYMBOL
(If applicable)

ONR

9. PROCUREMENT INSTRUMENT IDENTIFICATION NUMBER

N00014-86K-0230

8c. ADDRESS (City, State, and ZIP Code)

800 N. Quincy Street
Arlington, Virginia 22217-5000

10. SOURCE OF FUNDING NUMBERS

PROGRAM
ELEMENT NO.
61153NPROJECT
NO.
RR04108TASK
NO.
4414444WORK UNIT
ACCESSION NO.

11. TITLE (Include Security Classification)

Investigation of Resonant AC-DC Magnetic Field Effects

12. PERSONAL AUTHOR(S)

Durney, Carl H., Janata, Jiri, Rappaport, Catherine, Kaminski, Mark, Bruckner-Lea, Cindy

13a. TYPE OF REPORT

Final

13b. TIME COVERED

FROM 5/86 TO 7/89

14. DATE OF REPORT (Year, Month, Day)

1989 July 10

15. PAGE COUNT

43

16. SUPPLEMENTARY NOTATION

17. COSATI CODES

FIELD

GROUP

SUB-GROUP

08

18. SUBJECT TERMS (Continue on reverse if necessary and identify by block number)

magnetic fields; phospholipid membranes, calcium binding,
cyclotron resonance

19. ABSTRACT (Continue on reverse if necessary and identify by block number)

Recently reported observations by others indicate that a combination of a weak dc magnetic field and extra-low-frequency ac magnetic fields can produce resonant effects in biological systems. Our studies of resonant magnetic field effects consist of three parts: (1) calculations aimed at identifying the basic mechanisms underlying the resonance, (2) measurements of the effects of combined dc and ac magnetic fields on the dc current through plain (containing no channels) planar phospholipid membranes, and (3) measurements of the effects of combined dc and ac magnetic fields on the binding of metallochromic dyes and calmodulin to calcium. The calculations have provided insight and a physical mechanism that explains both frequency and amplitude windows in an elementary model consisting of one charged particle in a viscous medium. The combined dc-ac magnetic fields did affect the dc current through planar phospholipid membranes, but not in every membrane, and not consistently at the same values of magnetic field strength and (OVER)

20. DISTRIBUTION / AVAILABILITY OF ABSTRACT

☒ UNCLASSIFIED/UNLIMITED ☐ SAME AS RPT ☐ DTIC USERS21. ABSTRACT SECURITY CLASSIFICATION
(U)

22a. NAME OF RESPONSIBLE INDIVIDUAL

Dr. Igor Vodyanov

22b. TELEPHONE (Include Area Code)

(202) 696-4053

22c. OFFICE SYMBOL

ONR

DD Form 1473, JUN 86

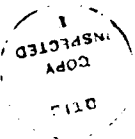
Previous editions are obsolete.

SECURITY CLASSIFICATION OF THIS PAGE

S/N 0102-LF-014-6603

BLOCK 19.

frequency. ~~We saw~~ no effect of the magnetic fields on the binding of metallochromic dyes and calmodulin to calcium. None of our measurements showed any resonant response like the cyclotron-like resonance reported in the literature in diatoms and lymphocytes.



Accession For	
NTIS GRA&I	<input checked="" type="checkbox"/>
DTIC TAB	<input type="checkbox"/>
Unannounced	<input type="checkbox"/>
Justification	
By	
Distribution/	
Availability Codes	
Avail and/or	
Dist	Special
A-1	

INVESTIGATION OF RESONANT AC-DC MAGNETIC FIELD EFFECTS

Carl H. Durney, Jiri Janata, Catherine Rappaport, Mark Kaminski, Cindy Bruckner-Lea. Electrical Engineering Department and Bioengineering Department, University of Utah, Salt Lake City, Utah 84112

ABSTRACT

Recently reported observations by others indicates that a combination of a weak dc magnetic field and extra-low-frequency ac magnetic fields can produce resonant effects in biological systems. Our studies of resonant magnetic field effects consists of three parts: (1) calculations aimed at identifying the basic mechanisms underlying the resonance, (2) measurements of the effects of combined dc and ac magnetic fields on the dc current through plain (containing no channels) planar phospholipid membranes, and (3) measurements of the effects of combined dc and ac magnetic fields on the binding of metallochromic dyes and calmodulin to calcium. The calculations have provided insight and a physical mechanism that explains both frequency and amplitude windows in an elementary model consisting of one charged particle in a viscous medium. The combined dc-ac magnetic fields did affect the dc current through planar phospholipid membranes, but not in every membrane, and not consistently at the same values of magnetic field strength and frequency. We saw no effect of the magnetic fields on the binding of metallochromic dyes and calmodulin to calcium. None of our measurements showed any resonant response like the cyclotron-like resonance reported in the literature in diatoms and lymphocytes.

1.0 INTRODUCTION

1.1 Goals of the Project

The purpose of this project is to explore basic mechanisms that might be involved in biological responses to resonant dc-ac magnetic fields such as those described below. We have made calculations for a simple model to explain the basic mechanisms that underlie the resonance response and to guide our experimental work. On the experimental side, we have measured dc current through planar phospholipid bilayer membranes (containing no channels) exposed to combined dc and ac magnetic fields. We also measured the effects of dc-ac magnetic fields on calcium binding using metallochromic dyes. In this report, the modeling and calculations are described first, followed by a description of our experimental work.

1.2 Background

Much work has been done in the last forty years to determine how electromagnetic fields interact with biological systems. Particularly in the last fifteen years, researchers have exposed many biological systems to various electromagnetic fields to study their responses. By far the majority of meaningful responses have been attributed to heating of the biological system by the electromagnetic fields. Although there are some responses that are thought to be nonthermal in nature, no one as yet has been able to relate responses to a consistent set of fundamental mechanisms of interaction, and the literature contains inconsistencies and questions about the observations that have been made. Perhaps this is not surprising in view of the great complexity of biological systems and the tremendous number of combinations of parameters that could be included in an experiment. For example, the frequency of the electromagnetic fields could vary over the spectrum from dc to 300 GHz. Couple this with the many possible combinations of electric and magnetic field strengths and configurations, and the number of experimental parameters is unmanageably large. Add to this the huge number of biological systems that could be studied, all the way

from the simplest in-vitro preparation to the complex behavioral patterns of whole organisms, and the matrix of possible experimental parameters is overwhelming.

In view of all this complexity, some recent observations are particularly intriguing for two reasons: first, they appear to indicate an effect that is perhaps more robust than many other observations, and second, they may be more readily explainable in terms of basic physical principles than most other observations. These recent observations are biological responses to combinations of dc and ac magnetic fields, apparently in some kind of a resonance reaction. Although dc magnetic fields, particularly that of the earth, have not usually been considered important in experiments involving electromagnetic radiation of biological systems, several recent publications may indicate a common underlying magnetic field resonance effect produced by combinations of dc and ac magnetic fields.

Jafry-Asl et al [1983] report a resonance effect on the dielectrophoretic yield in in-vitro preparations of yeast cells. They also found a resonance effect on the permittivity of the yeast cells.

Delgado et al [1982] and Ubeda et al [1983] exposed fertilized chicken eggs to pulsed magnetic fields and found strong developmental effects at field strengths of 1.2 microtesla and 12 microtesla when the pulse width was 0.5 ms and the repetition rates were 100 Hz and 1000 Hz. Although they did not give the information in their original published articles, the authors have stated in discussions that the effects did not occur unless the eggs were oriented east-west, which in their configuration meant that the applied ac magnetic field was perpendicular to the earth's magnetic field.

In other work that depends upon dc-ac magnetic fields, Blackman et al [1985] found that changes in calcium efflux occurred in chick-brain preparations only if the frequency of the applied ac fields was properly related to the dc magnetic field that was present. The authors suggested some sort of cyclotron resonance as the explanation for the required combination of dc-ac magnetic fields. This recent data showing the dependence of the change of calcium efflux on the dc magnetic field may possibly explain why others have not been able to replicate the data of Blackman et al, since apparently no one expected the dc magnetic field to be an important parameter.

More recently, Thomas et al [1986] have shown a strong behavioral effect in rats exposed to combined dc-ac magnetic fields. These investigators studied the effects of 60 Hz electric and magnetic fields on the abilities of rats to press levers within a narrow time window after a stimulus. They had found no significant effects in their previous studies in a laboratory ambient dc magnetic field of about 40 microtesla. However, when they adjusted the dc magnetic field to 26 microtesla, they found a significant effect on the rats' abilities to time the lever pressing. According to the authors, they chose the 26 microtesla field to correspond to the cyclotron resonance of a bare lithium ion at 60 Hz. Although the mechanism for this effect has not yet been identified, the effect is certainly a striking indication of the biological effects of magnetic field resonance.

McLeod and Liboff [1986] showed that the motility of a diatom preparation on a calcium impregnated agar substrate was highly dependent on the calcium concentration. Then they exposed the diatom preparation to the combination of a parallel dc and ac magnetic field and showed that the motility showed a strong resonance with frequency, centered about the cyclotron resonance frequency of a bare calcium ion. The resonance frequency was directly proportional to the dc magnetic field strength. These experiments are strong evidence of a biological response that is clearly related to resonant dc-ac magnetic field conditions.

Liboff et al [1987] exposed human lymphocytes suspended in a solution with radioactive Ca-45 ($^{45}\text{Ca}^{2+}$) to combined parallel dc and sinusoidal ac magnetic fields. In-

corporation of Ca-45 by the lymphocytes increased strikingly after one hour of exposure to fields when the ac and dc cyclotron resonant frequencies were equal to the frequency of the ac magnetic field of 14.5 Hz. The cyclotron resonant frequencies were calculated using the charge-to-mass ratio of the bare Ca-45 ion and the peak intensities of the applied ac and dc magnetic fields. The value of cyclotron frequency of 14.3 Hz or 21 μ T was used as the peak intensity for both magnetic fields. In contrast to the 16 Hz resonant peak found in the diatom experiments, the resonance response of Ca-45 incorporation occurred at 14.3 Hz, which is the resonant frequency corresponding exactly to the cyclotron frequency of the isotope of calcium. As the frequency of the ac magnetic field was adjusted to values around 14.3 Hz, a gaussian-like distribution in the amount of Ca-45 incorporated in the lymphocytes resulted. The 3-db bandwidth of this distribution was approximately 2 Hz.

There are a number of other reports of low-frequency magnetic fields causing significant biological responses, but with no mention of the possible role of the ambient dc magnetic field that is always present unless it is deliberately cancelled or shielded against. Since the dc magnetic fields required for the resonant effects described above are of the same order as a typical laboratory ambient magnetic field (the 26 microtesla used by Thomas et al [1986], for example), the laboratory ambient magnetic field could have played an unobserved role in many experiments. For example, Conti et al [1983, 1985] report that 3 Hz magnetic fields with intensities of 2.3-6.5 millitesla reduced the mitotic stimulation of human lymphocytes, and reduced the Ca^{2+} uptake by stimulated lymphocytes. It is conceivable that the frequency window they found within which ConA-induced blastogenesis was reduced by magnetic fields is due to a resonance with the dc magnetic field. This is only speculation, but since Blackman et al [1984] found that the dc magnetic field resonance significantly affected their measurement of calcium efflux, it is not entirely improbable.

Although cyclotron resonance for electrons in free space is familiar, few theoretical studies of effects of ac-dc magnetic fields on biological systems have been conducted. Chiabrera et al [1985] made calculations for a model of a charged ligand in the microenvironment of its binding site, which demonstrated a cyclotron-type resonance. Liboff [1985] made some calculations of cyclotron frequencies for ion species, and Mc Cleod and Liboff [1986] calculated the response of ions to ac-dc magnetic fields, but their calculations do not include the ac magnetic field, except in a very limited approximation.

We have made extensive calculations for a simplified model consisting of one charged particle in a viscous medium exposed to a parallel dc and ac magnetic field. The results are summarized below.

2.0 THEORETICAL CALCULATIONS

The details of our theoretical calculations are given in a recent paper [Durney et al, 1988]. In that paper we start with the simplest model, one charged particle in a viscous medium exposed to combined parallel dc and ac magnetic fields, along with the ac electric field induced by the ac magnetic field. We first solve the Lorentz force equation by a Runge-Kutta method to obtain the motion of the particle. Then we calculate the conditions for instability of the response by calculating the eigenvalues of the resolvent matrix of the equations of motion. Instability is defined as the condition for which the velocity and displacement of the particle increase without bound with time.

The results of the calculations may be summarized as follows:

1. The motion of the particle results from a combination of linear displacement by the electric field and bending of the path around the magnetic field lines. The typical resultant motion is a looping orbit that increases in size at or near resonance.

2. The model predicts "frequency windows." That is, for fixed values of the other parameters, strong response will be expected only for certain values of frequency.
3. The model predicts "amplitude windows." That is, for fixed values of the other parameters, strong response will be expected only for certain values of ac magnetic field strength.
4. When excitation is primarily due to an electric field alone, net charge transport will not occur. A charged particle in an ac electric field merely oscillates about its initial position.
5. When magnetic fields are present, net charge transport can occur. That is, the particle can be substantially displaced from its initial position, not just oscillate about it.
6. The resonance response is strongly affected by viscous damping. When the collision frequency of the particle with its surroundings is much greater than the frequency of the ac fields, no resonant response is observable.

The paper also explains how the physical mechanisms underlying the frequency and amplitude windows can be explained in terms of the synchronism of the particle with the electric field. When the particle's velocity is in the same direction as the electric field, the energy is transferred from the electric field to the particle and its velocity increases. The windows simply describe the conditions for which velocity of the particle would be in the same direction as the electric field most of the time during the orbit so that the motion builds rapidly.

It is remarkable that this simple model predicts the main features of the experimental observations of cyclotron-like resonance, amplitude and frequency windows. Results of the calculations have been very valuable in understanding physical mechanisms that might be related to the experimental observations.

3.0 MEMBRANE STUDIES

3.1 Rationale

The experimental observations described in the literature (see Section 1.1) are for resonant responses in biological systems. Because of the complexity of these biological systems, identifying the site of the basic interaction may prove to be very difficult. We have taken the approach, therefore, of beginning with the simplest, stablest system that might exhibit resonance response, and then proceeding systematically to more complex systems. Accordingly, we began with a simple planar phospholipid bilayer membrane preparation (containing no channels), as described below. We have measured the dc current through these membranes in the presence of combined dc and ac magnetic fields to study the effect of these fields on the membranes and to search for possible cyclotron-like resonance effects. We did find that the magnetic fields affect the membranes, but we did not find a resonance response.

Our planned next step was to introduce ion transport proteins into the membranes to see whether they would produce a resonance response. To this end, we prepared highly purified Ca-ATPase from rabbit sarcoplasmic reticulum and Na-K ATPase from rabbits. Both proteins were active as shown by the fact that when reconstituted into phospholipid vesicles, addition of ATP stimulated the active transport of both $^{45}\text{Ca}^{2+}$ and ^{22}Na into the vesicles. Time did not permit us to test membranes reconstituted with these channels to see if the transport of ions was affected by dc-ac magnetic fields.

Since the site of the interaction of the magnetic fields with calcium in the diatom and lymphocyte experiments [Smith et al, 1987; Liboff et al, 1987] has not been identified, we investigated the possibility that the magnetic fields might be affecting calcium binding,

but not necessarily in a membrane. We studied two cases, the complexation of two metallochromic dyes (murexide and arsenazo III) with calcium, and the binding of calmodulin to calcium. The binding of calmodulin to calcium provides a model of binding of an unsolvated ion, which is pertinent because the cyclotron resonance apparently affected the unsolvated ion in the diatoms and lymphocytes. As described later, we saw no effects in any of these experiments.

3.2 Membrane Properties

3.2.1 Biological Cell Membranes. Biological cells are surrounded by an outer membrane, barrier or wall that separates the internal cell constituents from the external environment. The membrane is a highly selective barrier made up of many ion- or chemical-selective pores, channels, or protein ion selective receptors. It is through these selective transport mechanisms that the cell communicates, induces reactions and survives in its environment.

Natural membranes are typically sixty to one hundred angstroms in thickness. Cantor and Schimmel [1980] suggest that the basic membrane structure is a phospholipid bilayer. Interwoven in this bilayer are many other chemical and biological components. These components, proteins and lipids, are very important to a fully functional cell and ultimately the host organism. The bilayer is very dynamic and is constantly passing chemical components between the interior and the exterior of the cell, adapting the cells to their environment and supporting a complex metabolism and reproduction. The membrane constituents are in constant motion; even the simplest cellular function depends on concerted changes in membrane composition or structure that can occur within milliseconds. Cantor and Schimmel [1980] state that a significant amount of evidence exists not only for lateral diffusion of lipid molecules in each of the monolayers but also movement between bilayer surfaces, referred to as "flip-flop".

Devaux and McConnell et al [1972] further reinforce the concept of cell membrane fluidity. The lateral pairwise exchange of phospholipid molecules occurs with a frequency of about ten million per second at twenty-five degrees Celsius. Exchange is only one type of movement reported. Diffusion of phospholipid molecules occurs at a rate of one to two micrometers per second, as suggested by Edidin [1974]. The fluidity of a cell membrane is believed to contribute significantly to a wide variety of biological functions. It may be involved in the ion transport mechanism between the cell membrane and the applied low-level electromagnetic fields.

Due to the chemical nature of the cell and its membranes, temperature changes play a critical role. Membrane constituents, lipid molecules, go through a phase transition from a highly organized state to a highly disorganized state as the temperature of the systems raises [Cantor and Schimmel 1980]. The disorganized phase is not characterized by an amorphous state but one with some structure still existing. In biological membranes this phase transition typically occurs over a broad temperature region, ranging from thirty to forty degrees Celsius. The phase transitions then would occur over the normal physiological temperature ranges, possibly sensitizing the membrane to certain effects, increasing or decreasing the probability of an observed response occurring. Individual lipids are believed to have narrow phase transitions, but since typical membranes are made up of many different kinds of lipids, the membrane phase transition is typically broader than for individual lipids.

3.2.2 Phospholipids. Several major kinds of lipids are found in nature. Phospholipids are the most common type of lipid found in biological membranes [Cantor and Schimmel, 1980]. These biomolecules are amphiphiles, containing both hydrophilic and hydrophobic regions. The hydrophilic component of a phospholipid is the polar head

group; and the hydrophobic regions consists of two hydrocarbon chains that form the two nonpolar tails. Studies have shown that there is a large variety of phospholipids that are distinguished by the type of polar head group, the lengths of the tails, and the number of double bonds in the two hydrocarbon tails.

Since the hydrophobic tails are much larger than the polar headgroups, phospholipids are insoluble in water and highly soluble in organic solvents. Water insolubility is expected as a result of the environment membranes typically exist in; otherwise structural integrity in a natural aqueous environment could not be maintained. High solubility of phospholipids in organic solvents is not expected nor is it required in the natural environment. The solubility characteristics are used to advantage in forming synthetic bilayer membranes in aqueous solutions; the lipid is dissolved in organic solvents and painted across an aqueous solution to form a membrane.

The polar head groups vary structurally with their molecular composition. This composition may or may not allow a net charge to be associated with the head group, which is very important for surface interaction and stability [Cantor and Schimmel, 1980]. The head groups arrange themselves so as to form the membrane surfaces, both interior and exterior to the cell. Cations in the electrolyte can then bind to the negatively charged moieties on the polar head groups.

The calculated strength of the cation binding for 1:1 association is greatest for Mg^{++} , followed by Ca^{++} , Na^{+} and K^{+} [Cevc and Marsh, 1987]. The binding strengths for cations surrounded by a hydration shell of water and for unhydrated cations are predicted to be the same order of magnitude; however neutron diffraction measurements have shown that unhydrated Ca^{++} binds to the phosphate groups of phosphatidylcholine bilayers [Cevc and Marsh, 1987]. Divalent cations are believed to interact strongly with the phosphate groups of neighboring lipids to form a kind of stapling-like lateral stabilization of the bilayer.

3.2.3 Planar Black Lipid Membranes. We chose planar black lipid membranes for experimental studies of magnetic field effects on membranes because they are the simplest known models of naturally occurring membranes. We began with plain membranes not containing channels with the intention of adding channels later. At the end of the contract period we had successfully prepared the channels, but not incorporated them into the membranes.

In-depth studies of thermodynamic principles governing the formation of phospholipid bilayers have provided an explanation for their spontaneous formation in aqueous solutions [Cantor and Schimmel, 1980]. The formation of lipid bilayers from phospholipids is attributed to the hydrophobic affect and to the sizes of the polar headgroups relative to the hydrophobic tail regions of the lipids. Since the polar headgroups favorably interact with water, they orient to the water interface and the hydrophobic tails form the interior of the structure. This process is driven by an increase in entropy of the water surrounding the lipid [Stryer, 1975]. When a hydrophobic molecule is in water, an ordered clathrate structure of hydrogen-bonded water will surround the nonpolar molecule. The structure of water around a hydrophilic species is less ordered, so the entropy (or disorder) of the water is greater around the hydrophilic molecule [Israelachvili, 1985]. The formation of planar bilayer structures rather than micelles (spheres with hydrophobic interiors) or other structures from phospholipids is due to the relatively large hydrophobic region that contains two tails, and is about the same width as the polar headgroup. In contrast, amphiphiles with only one hydrocarbon tail usually form micelles with the tails oriented radially inward and the headgroups oriented toward the water.

Although hydrophobic interactions are the primary driving force for membrane formation, other forces are also involved. Van der Waal forces are present between the hydrocarbon tails, with electrostatic and hydrogen bonding interaction between the polar head groups and water molecules. Spontaneous formation of the bilayer membrane results from all of these chemical interactions or binding forces.

Mueller and Rudin [1969] have outlined a theoretical thermodynamic cycle for forming a black lipid film across a 1-mm hole in a partition separating two aqueous compartments. Once the lipid is spread across the aperture, a relatively thick (when compared to the thickness of the membrane) film is formed. The film then undergoes tension since the lowest free-energy state of the system is in the bulk phase torus. The torus is around the rim of the aperture, composed of lipid material. Gravity then begins to cause the lipid material to drain down towards the lower torus allowing two surface monolayers of the lipid film to form at some point external to the torus region. A bilayer then forms at this point and then spreads, increasing the area of the bimolecular structure. If the bilayer is strong enough to withstand the surface tension of the torus, a stress to strain equilibrium is reached in which the surface free energy of the torus equals the surface free energy of the bilayer, and then the bilayer area remains essentially at a fixed value. If this condition is not met, the bilayer breaks. All the lipid is then drawn to the torus, which is the minimum energy configuration.

The standard approach is to dissolve the lipid substance in organic solvents and then paint the solution across the aperture in an aqueous solution. There is concern that some of the organic solvent may remain in the hydrocarbon tail formations, resulting in migrating solvent bubbles in the bilayer. The bubbles may then move around in the bilayer, resulting in measurable noise and/or instability in the BLM. This may explain some inconsistencies in our data. Since the bilayer is stretched across the aperture in a drum-like structure, it is very sensitive to vibrations, which can affect the dc current through the membrane.

The thickness of the bilayer depends upon the length and stiffness of the long nonpolar hydrocarbon chains. Measurements of the membrane thickness using electron microscopy, light reflectance methods and capacity [Mueller and Rudin, 1969] show that phospholipid membranes range from sixty to one hundred angstroms in thickness.

Asolectin (trade name), consisting of five different soybean phospholipids was purchased and used in making the bilayer membranes. The phospholipid composition of asolectin as determined by quantitative thin-layer chromatography [Miller and Racker, 1976] was: phosphatidylcholine 40%, phosphatidylethanolamine 33%, phosphatidylinositol 14%, lysophosphatidylcholine 5%, and cardiolipin 4%. Asolectin was stored in a tinted glass container and refrigerated. Argon or nitrogen gas was used to purge the open space of the container above the asolectin crystals to remove oxygen and other integrative gas molecules from the container. These precautions were taken to help retard the aging or oxidation process of asolectin. The lipid solution used to brush the phospholipid film over the aperture of the device was made by dissolving asolectin in decane solvent. All solvents and solutions were stored in glass containers. When the lipid solution was not in use, it was always purged with argon and stored in a freezer compartment.

Lipid solution concentrations as low as ten mg/ml (asolectin/decane) and as large as fifty mg/ml were used in forming membranes. No distinct differences were observed in membrane properties when the lipid solution concentration was within this range. However, it appeared more difficult to form a film across the aperture when using a lipid solution with a concentration near the lower limit of the range. Hence the standard concentration used was thirty mg/ml.

3.3 Experimental Apparatus and Methods

3.3.1 BLM Fixture. Following guidelines originally outlined by Mueller and Rudin [1962], a fixture in the form of a Lucite cube having two compartments separated by a partition was built to measure electrical conductivity and capacitive properties of bilayer phospholipid membranes (Fig. 3.1). Lucite provides the necessary structural rigidity and high resistivity, and is transparent enough to allow viewing of the membranes. A 1-mm hole was machined in the partition with the thickness of the partition directly around the hole kept to a maximum thickness of 1 mm. Both compartments were filled with an aqueous (electrolyte) solution up to a level of one to two millimeters below the top of the Lucite fixture. The solution contained selected ion species to facilitate electrolytic conduction. Recessing the water level below the top of the container helped to reduce the possibility of the formation of an unwanted salt bridge across the top of the partition and between the two aqueous compartments, which could result in erroneous electrical measurements.

Cleaning of the fixture before the electrolyte was added to each compartment was essential. Great care was taken not to scratch the surface area around the septum where the membrane formations occurs. Two methods were used to clean the Lucite compartments.

The first method consisted of soaking the fixture in a weak solution of detergent for at least ten hours. This helped to dissolve any organic molecules attached to the surface of the Lucite. Then the detergent molecules were removed by soaking the fixture in bidistilled water for thirty-minute time periods and briskly rinsing the fixture in water after each period. The soak and rinse cycle was carried on for at least two hours. The fixture was then dried by purging it with either nitrogen or argon gas for several minutes.

The second method used in cleaning the apparatus involved scrubbing very lightly the walls and aperture of the fixture with methanol using a fine brush. After rinsing several times with methanol, the fixture was repeatedly rinsed in bidistilled water five to ten times. It was then dried as in the previous method, purging it with nitrogen or argon gas. After drying was completed, the apparatus was accepted as having been cleaned and prepared for further steps in the bilayer formation. Since no differences in membrane properties were observed with either method, both methods were used. The second method was preferred, however, since it was less time consuming.

3.3.2 Fixture Pretreatment. Previous to the formation of a bilayer, the aperture and surrounding area on the surface of the septum that separates the two compartments of the fixture were preconditioned (pretreated) by brushing the lipid solution on the aperture and surface of the Lucite septum immediately around the hole. This layer was then allowed to dry for one hour. Without pretreatment, either the phospholipid membrane did not form or it lasted for only several minutes before spontaneously breaking.

Many factors contributed to membrane stability, lifetime, and properties of the bilayer membranes. Pretreatment of the septum and aperture walls is a major one. Others include: (1) allotted time for the pretreated area to be exposed to argon or open air before electrolyte is added to the compartments, (2) how much of the area around the aperture was pretreated, particularly whether or not the inner wall of the hole was pretreated.

Except for length of time, variations in pretreatment did not seem to affect membrane characteristics. For example, no differences were noticed in the membrane characteristics if the pretreated fixture was purged in argon and kept in the dark during the drying phase of the process or if the fixture was left in open room air in the presence of fluorescent room lighting. At least fifteen to thirty minutes was required for the pretreated area to dry in order for the pretreatment process to reach its optimum effectiveness in forming a bilayer. Longer periods of time were not noticeably detrimental to the effectiveness of the process.

Using a dissecting scope (X30 power), it was found that under certain conditions the phospholipid film applied across the hole would balloon in a convex shape outward

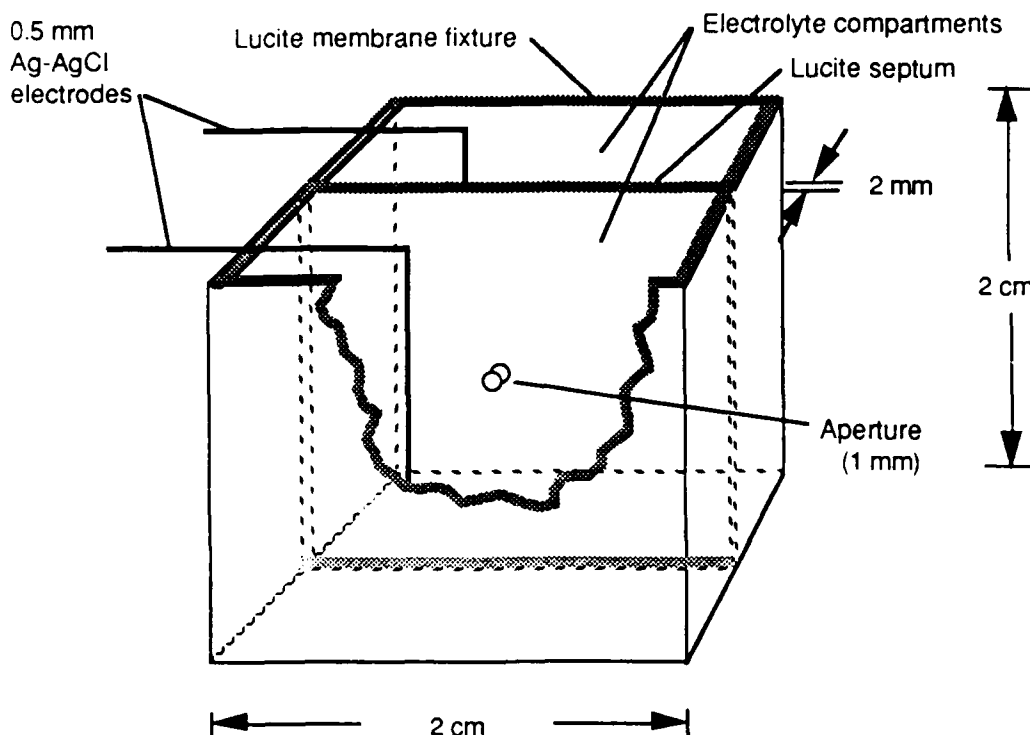


Fig. 3.1 Membrane chamber. The cube, made of Lucite plastic is separated by a partition with a hole drilled in the center. The membrane is painted on a 1 mm diameter hole in the septum separating the electrolyte compartments. The thickness of the septum was reduced to 1 mm within a 6 mm diameter circle around the hole. None of the joints separating the two compartments were glued.

from the fixed Lucite septum and the attachment of the film to the Lucite would migrate radially away from the center of the aperture. Ballooning occurred more readily when liberal amounts of lipid solution were applied over at least a 10-mm radius around the center of the aperture. Hydrostatic pressure difference between the two compartments is one possible explanation for ballooning, since dipping the brush into one chamber to form the membrane would cause a difference in the volume of the electrolyte in the two chambers when the brush was removed after the membrane was formed. Ballooning increased lipid film capacitance and conductance by as much as two fold (sometimes more), and seemed to cause drift in the electrical conductance and capacitance. Some of the variations in our data may have been caused by the effects of ballooning.

It was also observed through the dissecting scope that when the inside surface of the hole through the septum was pretreated with lipid, the bilayer lipid film could migrate back and forth across the width of the septum. This type of motion is also believed to have caused inconsistencies and magnitude drift in the measured electrical parameters of the membrane.

Therefore several guidelines were followed which were considered important in order to decrease drift and to obtain the highest stability in the electrical characteristics of each membrane.

1. A minimum of thirty minutes was allowed for the preconditioned area around the aperture to be exposed to either argon or nitrogen gas or to open air; our standard evolved to a one-hour pretreatment time in open air to aid in reducing variables.
2. Careful application of the lipid during the pretreating process was made to prevent the inside surface of the aperture from being coated with lipid. This appeared to prevent the membrane from migrating transversely across the thickness of the septum.
3. The area radius around the hole center, coated with lipid during preconditioning, was limited to a maximum of approximately three to five millimeters. When this precautionary measure was made, a higher percentage of membranes exhibited a capacitance value similar to what would be expected (approximately 2 nF), and consistent dc current of 0.6 to 0.1 pA with a 1 mm diameter aperture.

These techniques were developed over a period of six months to improve membrane stability, lifetime, and consistency.

3.3.3 Forming the Membranes. The Mueller-Rudin brush technique utilized in this study for making black lipid membranes is a relatively simple process. The technique, however, has some drawbacks that may cause inconsistencies in membranes. As has been stated, the lipid solution used to form the bilayer includes a hydrocarbon solvent (we used decane). Henn et al [1967] have concluded from electron microscopic observations and direct measurements of membrane composition that the bilayers contain significant numbers of decane bubbles. They concluded that because of this, transient distortions in the structure of the membrane and its thickness may result. If this is true, transients in the electrical capacitance and conductance of the membrane may occur. Another drawback is the existence of the torus or annulus which surrounds the bilayer membrane and is located at the point of attachment around the rim of the aperture of the Lucite septum. The volume of the torus cannot be regulated, which causes variability.

Electrolyte was first added to each compartment to a level approximately 2 mm below the top of the Lucite fixture and a silver chloride electrode was inserted into each compartment. After dipping the tip of a brush into the lipid solution, pressure was applied to the tip of the brush and against the partition separating the two compartments. The lipid solution was then spread across the aperture while it was submerged in electrolyte. This procedure was performed without the use of the magnifying dissecting microscope because of prohibitive physical difficulty in using the microscope in close quarters to the apparatus.

However, after the formation of the membrane, the microscope was used (hand held) to visually check for air bubbles trapped in the lipid solution within. As a result of this technique the volume used to pretreat the aperture and to paint lipid across the aperture was controlled by the brush used and viscosity of lipid solution. The brushes were very fine paint brushes ("101 Winsor & Newton") with the bulk of the hairs removed. The pretreatment brush contained between ten and fifteen hairs, and the membrane brush contained between two and four hairs. The brushes were typically dipped in the lipid only to apply the pretreatment or paint the membrane.

3.3.4 Electrodes and Capacitance Measurements. The electrodes inserted into each compartment of the fixture served as a transducer which converted ionic current in the electrolyte solution to electron current in the electrodes. It is beyond the scope of this report to review in detail all the underling theory dealing with the electrode-electrolyte interface.

A dc voltage potential of 60 mV dc when using 1 mM CaCl_2 and 20 mV dc when using other ions was applied across the two electrodes, just previous to the membrane being made. Before the membrane was formed, the dc voltage produced a current of approximately 500 nA dc due to the resistance of the electrolyte. When the lipid film formed across the aperture, the dc current decreased to an extremely small value, typically less than one picoampere.

A Wavetek generator was used to superimpose a triangular time varying voltage onto the dc voltage to measure the membrane capacitance. The resulting ac current consisted of a capacitive and a resistive component. Without the presence of a lipid film, the magnitude of current was relatively large due to a small value of resistance (100K ohms) and its waveform shape was nearly identical to that of the applied triangular excitation voltage. With the formation of a lipid film, the resistance increased to approximately 10^{10} to 10^{11} ohms, and therefore the capacitive current became by far the major electric current component. With a lipid bilayer in place, the membrane capacitance resulted in a displacement current characterized by a square waveform (the current through a capacitor is proportional to the derivative of the voltage across the capacitor). The square waveform of the resultant ac current was monitored by an oscilloscope connected to the analog output of the electrometer. After the presence of a lipid film had been detected, capacitance measurements were used to monitor thinning of the bilayer and the formation process of the bimolecular structure.

From capacitance and conductance measurements on numerous membranes made in our study, mature asolectin bilayers formed using the Lucite fixture were characterized. These values were also compared with those measured by Ashcroft [1980]. This provided a comparison of capacitance and conductance values when making lipid bilayers, assisting in the determination of whether or not the lipid film had actually thinned into a bilayer membrane.

Until the membrane had thinned, resulting in an acceptable capacitance, no magnetic fields were applied. This would take approximately one hour. During this thinning process, conductance was also monitored by switching the Wavetek generator source from a triangular voltage waveform to strictly a dc voltage. The dc electric current was then measured by the electrometer. Since large conductance changes and transients occurred during the thinning of the membrane, no data was taken during that time. It was observed that with a dc potential applied before the membrane was present, polarization of the electrodes was occurring. The polarization of the electrodes would then affect the applied dc potential after the membrane was painted. This resulted in a slight potential that opposed the applied potential, effectively reducing the total potential and the measured current. As the applied potential discharged the polarizing potential, the dc current slowly increased to a steady-state value.

3.3.5 System Overview. Figure 3.2 shows the experimental arrangement and instrumentation used for exposing the bilayer membrane to externally applied magnetic fields and measuring the dc current through the membrane. A Hewlett Packard 9000-300 series computer work station was used to set values of the ac and dc magnetic fields and collect the data. The data and instrument instructions were sent to and from the computer through the standard IEEE-488 bus. The computer was also used to analyze and compare the data. This computer-controlled system allowed us to obtain a great amount of data that would have been impossible to record by hand.

The experimental procedure consisted of applying a dc voltage across the membrane and then monitoring the resulting dc electric current through the membrane. A Wavetek 185 function generator was used to apply a dc potential of 60 mV dc or less

across the membrane. This function generator would also apply a triangular voltage of 10 mV ac peak-to-peak (p-p) during the first hour of the membrane formation to measure membrane capacitance. Capacitance measurements were used to detect when the lipid film had thinned into a bimolecular structure, and to what extent the thinning had taken place.

The resultant dc current through the membrane was measured by a Keithley 617 electrometer. The electrometer had a digital low-pass filter built into it as a result of the analog to digital converter. The effective bandwidth of this device on the 2.0 pA scale was 0.40 Hz. This helped reduce the background noise and current fluctuations. Its analog output had a larger bandwidth of approximately 400 Hz. Signal averaging was used to improve the data.

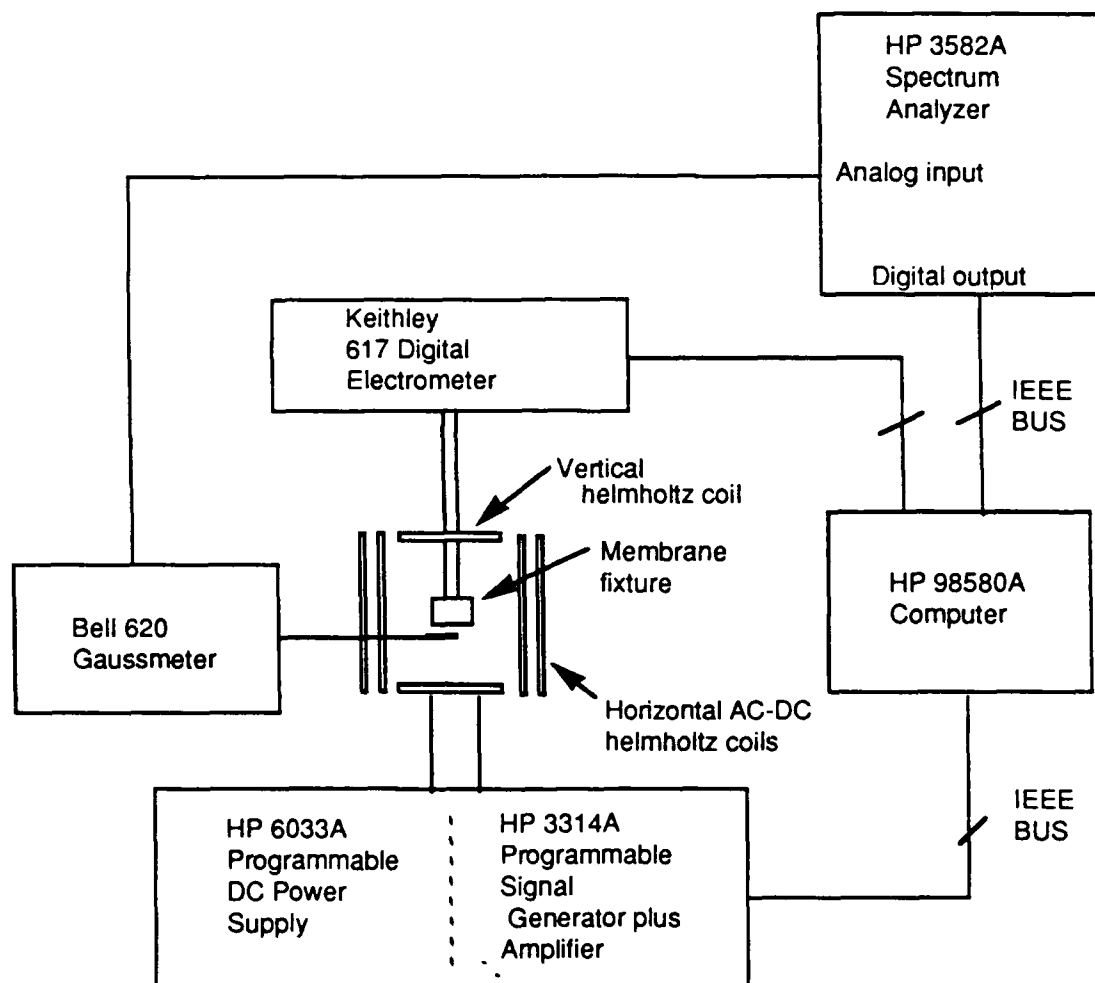


Figure 3.2. Block diagram of the instrumentation system.

3.3.6 Temperature Characterization of the Electrolyte. When fields were applied for a period of one to two hours, the temperature of the air inside the chamber increased slowly and monotonically about three degrees Celsius and the temperature of the electrolyte increased about two degrees Celsius. Since phospholipid membranes are sensitive to temperature [Cantor and Schimmel, 1980], a change of one or two degrees could affect the dc current significantly, especially if the temperature were near a phase transition

of the membrane. Our temperature measurements indicated, however, that the phospholipid membranes that we used did not have a well defined phase transition temperature, presumably because the membranes consisted of a mixture of phospholipids. For some experiments, we controlled the electrolyte temperature with a temperature-controlled water bath surrounding the membrane chamber, but we found that the vibrations due to the circulating water had a greater effect on the membrane current than the temperature variations, so we discontinued use of the water bath. Since our temperature measurements showed that the temperature changed very slowly, we feel that the temperature changes had a negligible effect on the membrane response, and in particular that the changes that we observed in dc current with applied magnetic fields can not be attributed to temperature effects.

3.3.7 Magnetic Field Generation. The horizontal components of the ac and dc magnetic fields were independently generated by electrical current in two separate pairs of Helmholtz coils. The individual coils in each pair were connected together in a Helmholtz-like configuration. One Helmholtz pair was positioned inside the separation distance of a second pair, both having a common axis parallel to the horizontal component of the earth's magnetic field vector.

The coil radii and separation distances were selected to produce acceptable magnetic flux uniformity and intensities and to provide enough space for the membrane chamber. The coils were wound with 256 turns of B&S 18-gauge copper enameled magnet wire around the perimeter of plexiglas cylinders having radii of 12.5 cm. A Hewlett Packard 3314A programmable function generator was used as a voltage source for an audio amplifier that provided electric current amplification needed to drive the coils. A sinusoidal time varying current from the amplifier was used to excite the inner horizontal Helmholtz coil to generate the ac magnetic flux required, with a magnitude corresponding to the desired cyclotron resonant frequency f_{c1} at the desired frequency f . f_{c1} is the cyclotron frequency corresponding to the ac magnetic field strength; it is defined by $f_{c1} = qB_1/2\pi m$, where q is the charge and m is the mass of the particle, and B_1 is the ac magnetic field strength.

A Hewlett Packard 6033A programmable dc power supply was used as the dc current source applied to the outside set of horizontal coils to generate the dc magnetic field. Having B_0 parallel to the geomagnetic vector allowed adding to or subtracting from the geomagnetic field to produce the desired net horizontal dc magnetic field component corresponding to the cyclotron frequency f_c .

A third Helmholtz coil pair was used to adjust the vertical component of the dc magnetic field by adding to or subtracting from the vertical component of the geomagnetic field. It was excited by a Hewlett Packard 6203B dc power supply.

A Bell 620 gauss meter was used to measure the magnetic field magnitudes at the location of the membrane. The maximum intensity of dc magnetic flux density generated in the experiments was 260 μT , which required 1.2 amperes of source current. The majority of experiments used a fixed peak intensity of ac magnetic field of 130 μT , which corresponds to a calculated cyclotron frequency based on the charge-to-mass ratio of a bare calcium ion of 100 Hz, while different ion experiments used intensities as low as 117 μT and as high as 170 μT . The oscillation frequency of the ac magnetic field was held at 100 Hz, but it could be varied if desired. The magnetic flux at the location of the membrane was uniform within 0.3 of a percent along a 1 mm distance on any of the three orthogonal axes. Ambient noise, detected in the earth's magnetic field magnitude, including frequencies from dc to 60 Hz, was less than 150 nT.

The membrane fixture was physically moved until the aperture was centered on the horizontal axes of the coaxial Helmholtz coils. The fixture was rotated until the plane of the septum wall and aperture was perpendicular to the coil axes. The fixture was then moved

along the horizontal axes, to the center location of the Helmholtz coils where the maximum uniformity of the magnetic field was found. Then a permanent support fixture was designed to stabilize the alignment. Most of the experiments were done with the ac and dc magnetic fields parallel to each other and perpendicular to the membrane.

Since the ac magnetic field unavoidably induces voltages in the instrumentation, the ac magnetic field strength and the ac frequency were set at selected values and the dc current through the membrane was measured as the dc magnetic field strength was changed by small increments. Any changes in dc current with dc magnetic field would not be due to changes in induced voltages since a dc magnetic field does not induce voltage.

An aluminum box connected to a stable earth ground was placed around the coils to shield against noise, which was necessary when measuring such small currents, typically less than 1.0 pA. The ac magnetic fields induced currents in the aluminum box, which in turn produced ac magnetic fields that subtracted from the ac magnetic fields produced by the Helmholtz coils and made the measured ac magnetic field less than the calculated ac magnetic field. A Bell 620 gaussmeter was used to monitor the magnetic field strengths and adjust them to the desired values.

3.3.7 Membrane Electric Current Measurements. The current was produced by an external dc voltage source of 65 mV dc or less, connected across two Ag-AgCl electrodes (Figure 3.2). It was observed that the lower the applied dc potential, the less stress induced upon the membrane and the smaller the dc current, resulting in the signal approaching the noise level of the system. The membranes also appeared to thin faster with higher applied dc potentials, but membranes formed with higher dc potentials also seemed to be less stable. For our experiments we typically used 60 mV dc for 1 mM CaCl_2 and 20 mV dc for the other ions tested. The electrometer was connected in series with the low-impedance dc voltage source and the lipid bilayer to monitor the electric current. The measured and sampled analog values of dc electric current through the bilayer were digitized and then further processed by the external controlling computer.

As the fixed value of ac magnetic field (B_1) (between 120 μT and 170 μT) was applied and the dc magnetic field (B_0) was incremented through a selected interval of field intensities (0 to 260 μT), the membrane current was monitored for significant changes that may have been due to field effects. Control runs consisting of dc current measurements without applied magnetic fields were made before and after field exposure. Many of the lipid membranes formed were characterized by a high degree of instability in the dc current. It was, therefore, often difficult, if not impossible, to distinguish whether the deviations in the current were due to membrane instabilities or field effects.

3.4 Results

Measurements of dc current in the presence of applied ac and dc magnetic fields were made with the following electrolytes: 1 mM CaCl_2 , 150 mM NaCl, 150 mM KCl, 150 mM LiCl, and 150 and 1 mM MgCl_2 . The concentrations were chosen to be similar to those in the biological environment and to allow comparison of the effects of divalent and monovalent ions on membrane characteristics.

3.4.1 Typical Membrane Responses. Figure 3.3 shows a control run for the dc current through a resistor having approximately the same resistance as a membrane. These data show that the system is acceptably stable, with reasonably low noise. Figure 3.4 shows the dc current through the same resistor for a simulated field run. The data in Fig. 3.4 are very important because they show that the application of the magnetic fields introduces no artifacts in the dc current due to, for example, voltages induced in the wires or instruments.

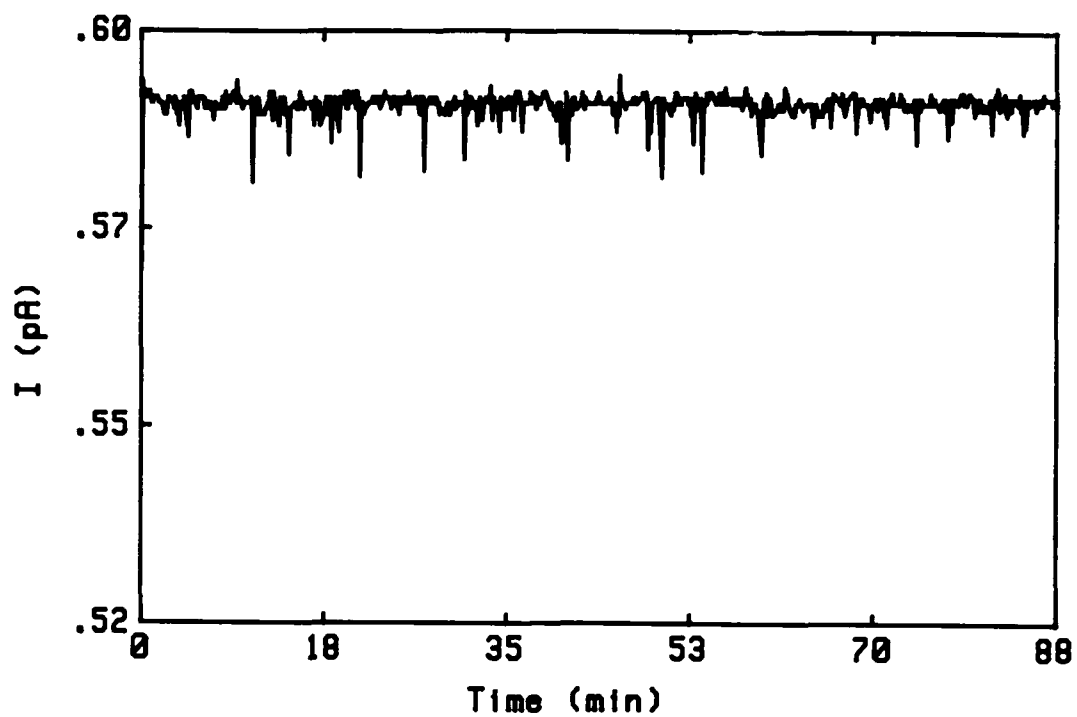


Fig. 3.3. Control run with a resistor in place of the membrane.

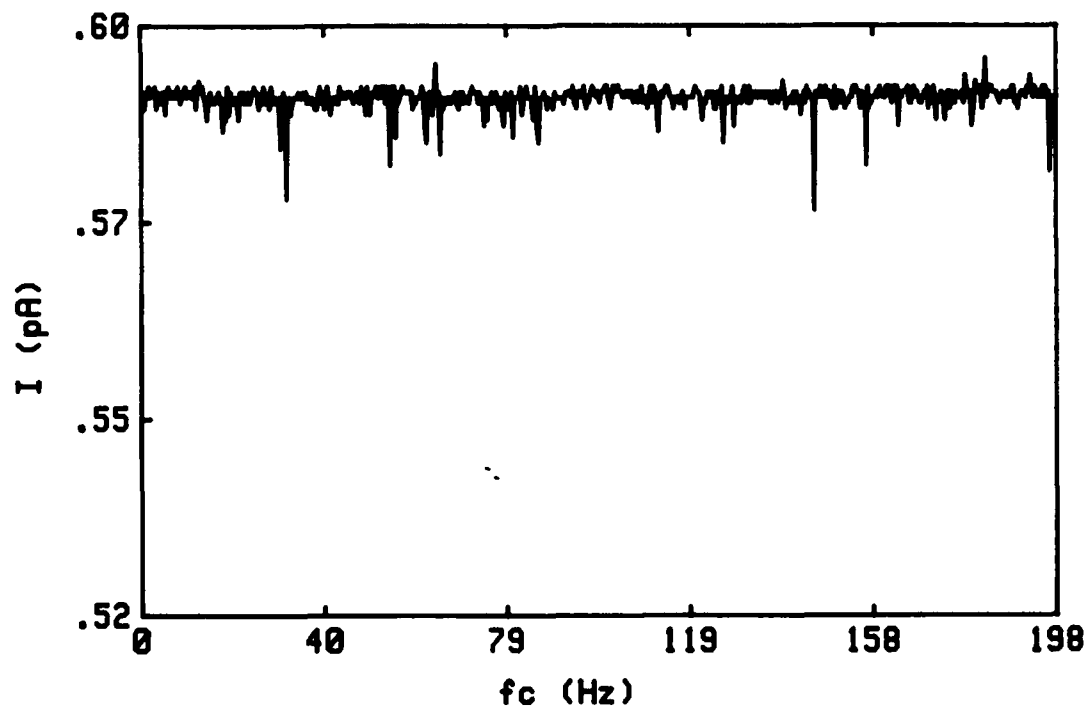


Fig. 3.4 Field run with a resistor in place of the membrane.

Figure 3.5 shows a control run for one of the more stable membranes. To characterize the stability of membranes, we have calculated the ratio of the standard deviation to the mean value of dc current. For the membrane of Fig. 3.5, this ratio is 0.04, a relatively low value. By way of contrast, Fig. 3.6 shows a control run for a membrane after magnetic fields had been applied and removed. In this case the standard deviation is 7.295 pA and the mean value is 30.77 pA for a ratio of 0.24. This data is an example of a frequent observation that the applied magnetic fields seemed to affect the membranes so that control runs after the fields had been applied and removed showed increased levels of instability.

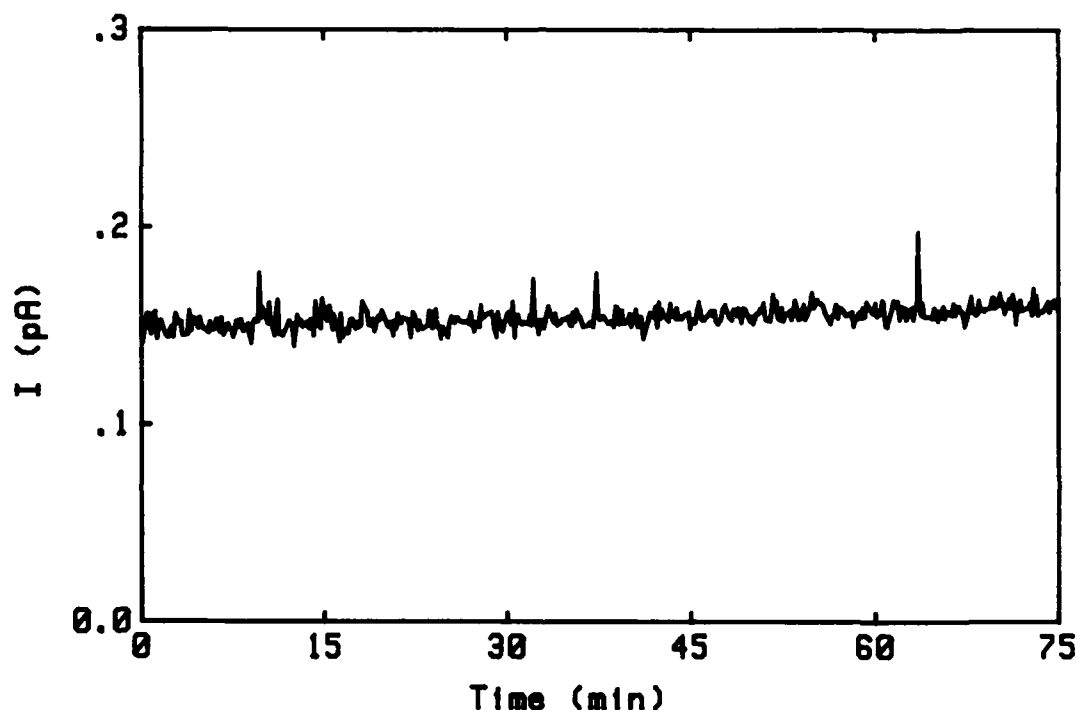


Figure 3.5 Control run showing dc current as a function of time. Electrolyte: 1 mM CaCl_2 . $V_{\text{dc}} = 60$ mV across the membrane. Standard deviation of the current is 0.0058 pA. Ratio of the standard deviation to the mean is 0.04.

Data for the first membrane in which we saw the magnetic fields affect the dc current is shown in Fig. 3.7. In this and subsequent figures, we have plotted the dc current versus the dc magnetic field strength, with the dc magnetic field strength expressed in terms of the cyclotron frequency for the bare calcium ion; i. e. $f_c = qB_0/2\pi m$, where q/m is the charge-to-mass ratio for the bare calcium ion and B_0 is the dc magnetic field strength. We also express the ac magnetic field strength in terms of the corresponding cyclotron frequency of the bare calcium ion: $f_{c1} = qB_1/2\pi m$. During the computer-controlled run shown in Fig. 3.7, the graduate student doing the experiment saw the change in the dc current that occurred for f_c greater than about 60 Hz. To verify that the magnetic fields

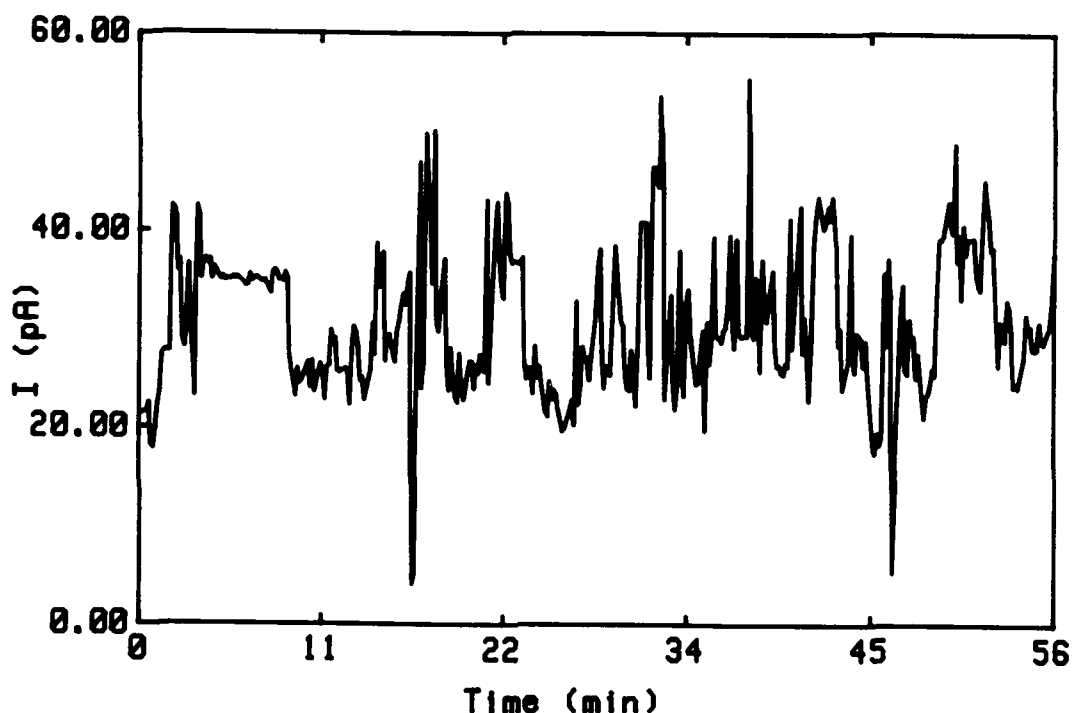


Figure 3.6. Control run showing dc current as a function of time. Electrolyte: 150 mM MgCl_2 . $V_{\text{dc}} = 10$ mV across the membrane. Standard deviation of the current is 7.295 pA. Ratio of the standard deviation to the mean is 0.24.

were causing the changes, he manually set the magnetic fields back to the values for which high current changes occurred (the computer had set the magnetic fields back to zero after the run was completed and the current had returned to about 0.6 pA). The current immediately increased to several pA, but not at a steady level; it fluctuated with an amplitude of 1 to 2 pA about the higher level. After about thirty seconds, he turned the magnetic fields to zero again. After several minutes the dc current returned to about 6 pA. Then he turned the magnetic fields on again, tuning them to get an increased current level. The level was even higher this time, with greater fluctuations. When he turned the fields back to zero, the current stayed high and the membrane soon broke. This demonstrates that the magnetic fields affect the current, but not in a way similar to the responses observed in the diatoms [McCleod and Liboff, 1986], for example, in which the response clearly occurred at the cyclotron frequency in a clearly resonant fashion. In our case the magnetic fields seemed to affect the membrane in some way that caused the current to change dramatically, but in a somewhat erratic fashion.

Figures 3.8 and 3.9 show two consecutive experimental runs on the same membrane. Although the magnetic fields seemed to change the current in each case, the two patterns of response were quite different. This membrane broke within five minutes after the data in Fig. 3.9 were collected. We often found that the membranes were less stable after the magnetic fields had been once applied.

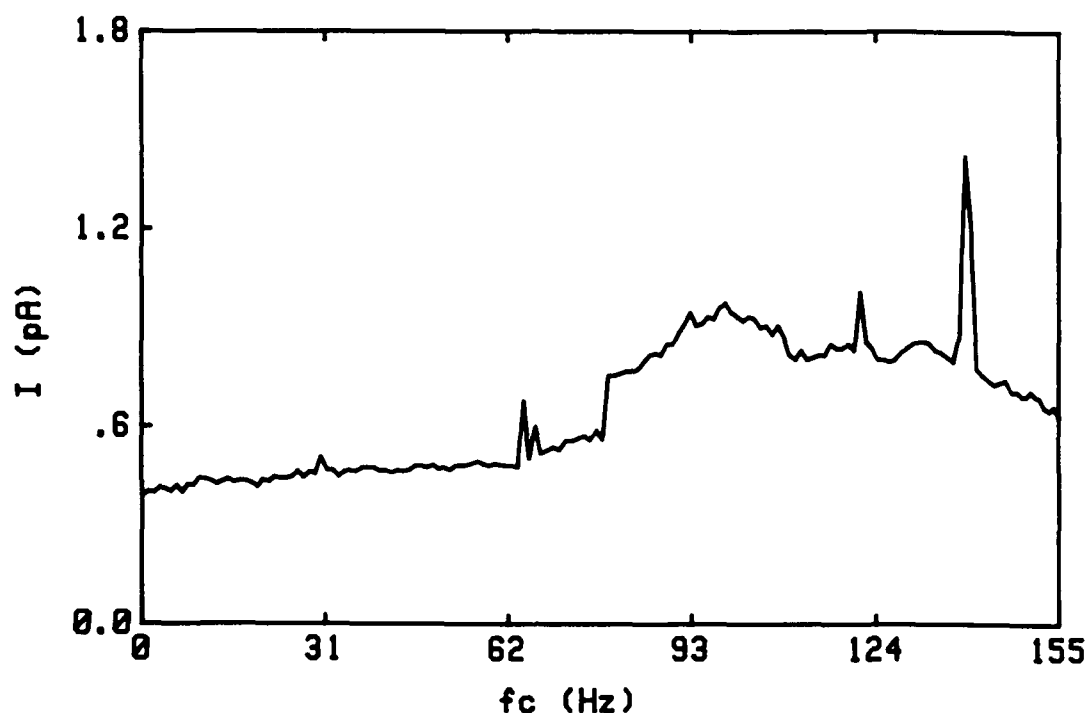


Figure 3.7. Field run showing dc current as a function of dc magnetic field strength calibrated in terms of the cyclotron frequency f_c (step size = 1 Hz). $f = 100$ Hz (frequency of ac fields), $f_{c1} = 95$ Hz (cyclotron frequency of ac magnetic field: $B_1 = 124 \mu\text{T}$). Electrolyte: 1 mM CaCl_2 . $V_{dc} = 65$ mV across the membrane. Standard deviation of the current is 0.2 pA. Ratio of the standard deviation to the mean is 0.306.

Additional examples are shown in Figs. 3.10 through 3.13. The data in these four figures were sequentially obtained using one membrane. Figure 3.10 shows a control run with no fields previously applied. The ratio of the standard deviation to the mean value for these data is 0.159. Figure 3.13 shows a control run for the same membrane, but made after magnetic fields had been applied. For this case, the ratio of the standard deviation to the mean value was 0.387, which is more than double that of the first control run, illustrating again the apparent decrease in stability of the membrane after fields were applied.

The data for the field runs are shown in Figs. 3.11 and 3.12. The magnetic fields had little effect on the current the first time (Fig. 3.11), but a large effect the second time (Fig. 3.12). This unexplained variability in response was common.

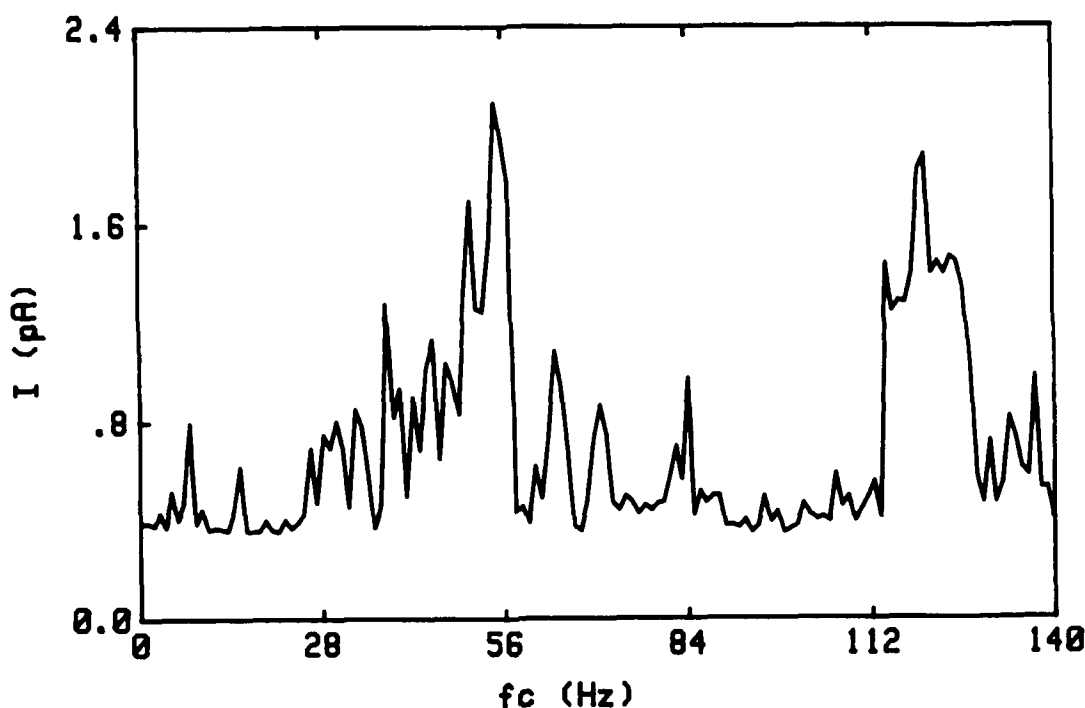


Figure 3.8 Field run showing dc current as a function of dc magnetic field strength calibrated in terms of the cyclotron frequency f_c (step size = 1 Hz). $f = 100$ Hz (frequency of ac fields), $f_{c1} = 100$ Hz (cyclotron frequency of ac magnetic field; $B_1 = 130 \mu\text{T}$). Electrolyte: 1 mM CaCl_2 . $V_{dc} = 65$ mV across the membrane. Standard deviation of the current is 0.383 pA. Ratio of the standard deviation to the mean is 0.563.

3.4.2 Summary of Results. It is not practical to show data for all the membranes for which we made measurements for all six electrolytes, and since the responses of the membranes were so variable, it is difficult to summarize the data to show in some compact way how the magnetic fields affected the membranes. The limited statistical data presented below gives some information about the overall effects, but not in a very quantitative or specific way. Nevertheless, the summaries below do show that the magnetic fields affect the membranes in some as yet unexplained way.

The lipid bilayer capacitance was used as a relative measure of how the membrane was thinning after being painted across the aperture. The capacitance would typically stabilize in the first thirty minutes after being formed. The ac potential was applied for the first 60 minutes during which time the membrane capacitance was monitored. Figure 3.14 shows the initial average membrane capacitance for all the ion concentrations used. The average value of capacitance varies only from 1.4 to 2.7 nF for the different ions. Assuming that the membrane completely fills the aperture (with no area occupied by the torus), the specific capacitances range from 0.18 to 0.34 $\mu\text{F}/\text{cm}^2$ for the different ions. If the torus were taken into account for each membrane, these values would be within the range of 0.3 to 1.3 $\mu\text{F}/\text{cm}^2$ measured for a variety of lipid systems [Tien, 1974]. This agreement indicates that the membranes in our experiments were indeed thinned to bilayers.

The dc current through the membrane changed significantly with both the species of ion and the ion concentration. Membrane stability and lifetime also varied significantly with ion species and concentration. The applied magnetic fields affected the dc current, but not in every membrane and not consistently at the same values of frequency and field strength, as observed in the cyclotron-like resonance response in biological systems.

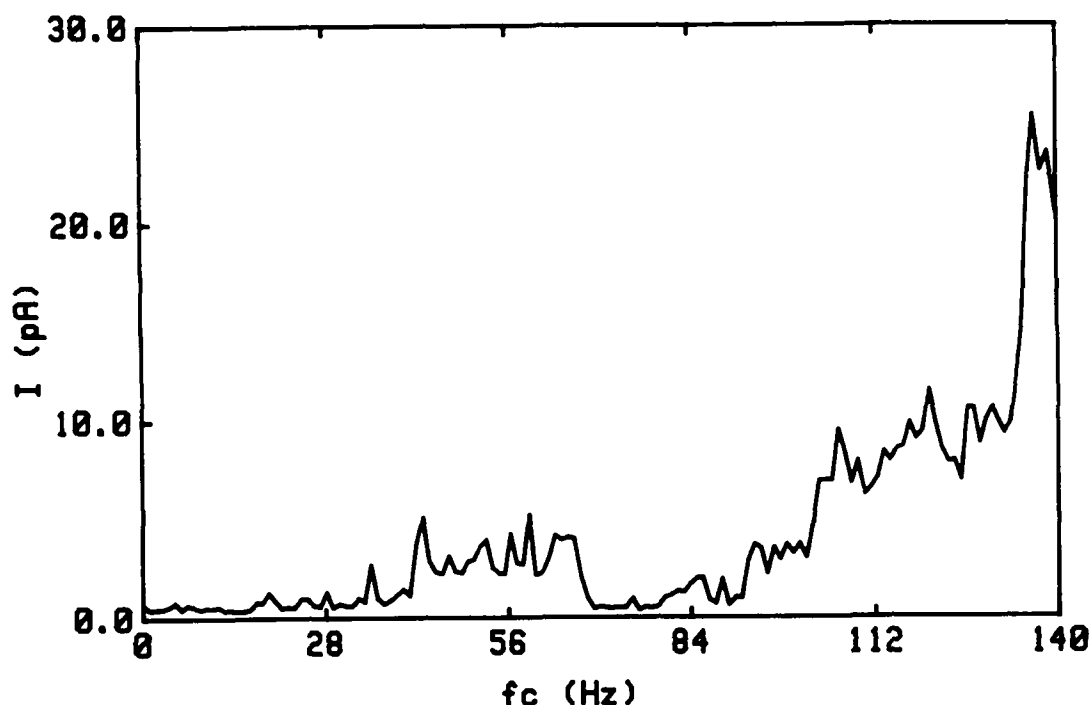


Figure 3.9 Field run showing dc current as a function of dc magnetic field strength calibrated in terms of the cyclotron frequency f_c (step size = 1 Hz). $f = 100$ Hz (frequency of ac fields), $f_{c1} = 100$ Hz (cyclotron frequency of ac magnetic field; $B_1 = 130 \mu\text{T}$). Electrolyte: 1 mM CaCl_2 . $V_{dc} = 65$ mV across the membrane. Standard deviation of the current is 5.0 pA. Ratio of the standard deviation to the mean is 1.2. These data are for the same membrane as in Fig. 3.8.

In measuring dc current in many membranes, we found that some membranes were so unstable and noisy (without magnetic fields applied) that measurements of dc current were meaningless. After considerable experience in making membranes, we found that a good criterion for judging a stable membrane was whether the mean dc current was below 10 pA, since invariably the membranes with a mean dc current above 10 pA were unstable and broke shortly after being formed. Therefore, in studying the effects of applied magnetic fields on the dc current, we included data only for those membranes for which the mean dc current was below 10 pA. Figure 3.15 shows the mean value of the initial dc currents as a function of the electrolyte composition for all the membranes with mean dc currents below 10 pA.

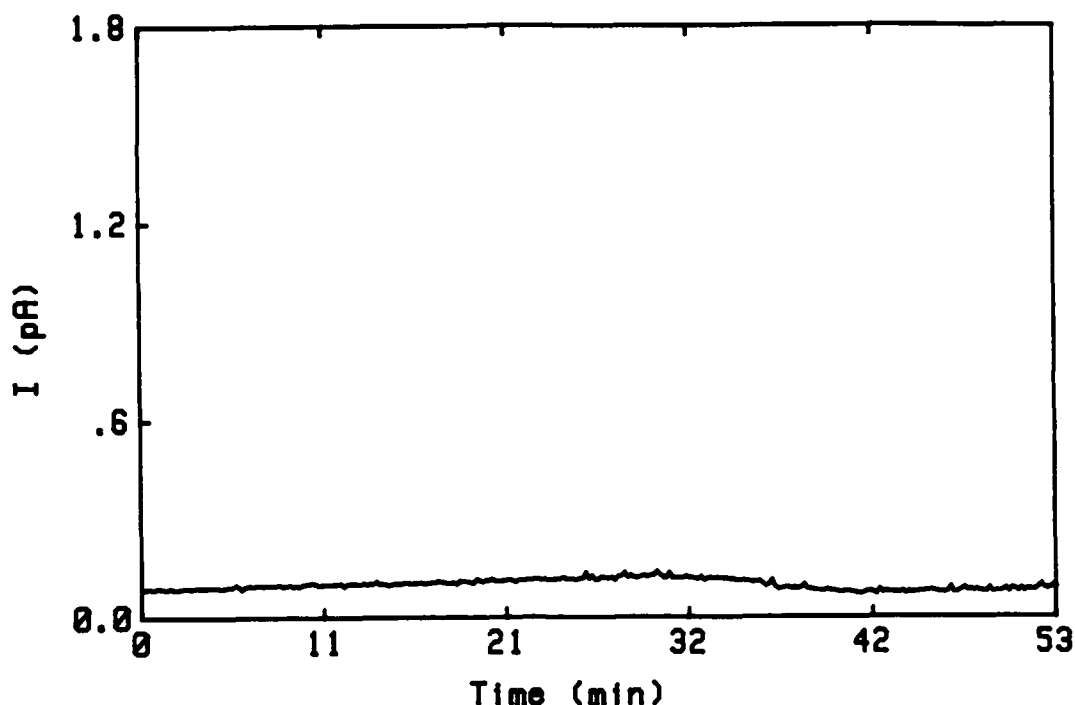


Figure 3.10. Control run showing dc current as a function of time. Electrolyte: 1 mM CaCl_2 . $V_{dc} = 60$ mV across the membrane. Standard deviation of the current is 0.016 pA. Ratio of the standard deviation to the mean is 0.159.

The membrane lifetime varied from seconds to twenty-four hours from the time the membrane was first formed until it broke, with the majority of them breaking within the first ten hours. The membranes usually thinned rapidly during the first hour after painting, as evidenced by a dramatic increase in the level of membrane capacitance and decrease in conductance. It was also during this maturing period that the greatest instability in the electric current was observed. Therefore data collected during the first hour of the life of the membrane were typically not used for analysis. Figure 3.16 shows the average age of the membranes (the number of files used is shown above the appropriate column) at the time of the field runs and control runs. Since field and control runs were conducted until each membrane broke, a larger initial age for the runs indicates that a membrane has a larger lifetime. The electrolyte had a significant effect on the age of the membranes. Membranes usually lasted longer with 1 mM CaCl_2 and MgCl_2 , and not as long with the 150 mM concentrations.

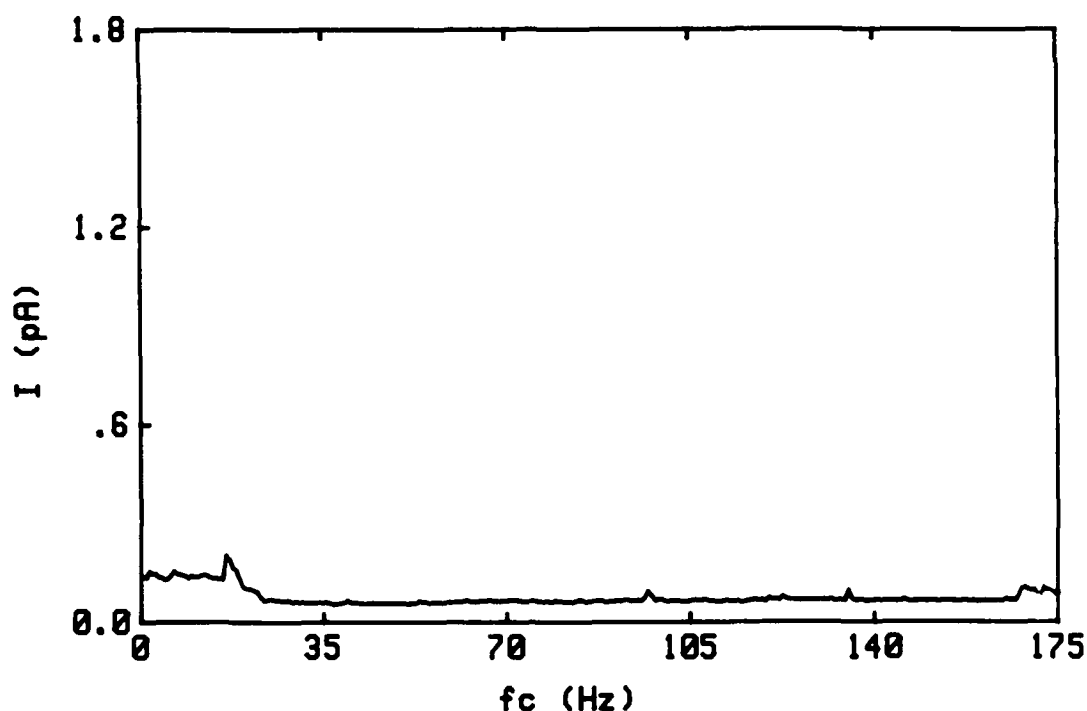


Figure 3.11 Field run showing dc current as a function of dc magnetic field strength calibrated in terms of the cyclotron frequency f_c (step size = 0.6 Hz). $f = 100$ Hz (frequency of ac fields), $f_{c1} = 100$ Hz (cyclotron frequency of ac magnetic field; $B_1 = 130 \mu\text{T}$). Electrolyte: 1 mM CaCl_2 . $V_{dc} = 60$ mV across the membrane. Standard deviation of the current is 0.027 pA. Ratio of the standard deviation to the mean is 0.352. Same membrane as in Fig. 3.10.

Figure 3.17 shows how the ratio of the standard deviation to the mean value of dc current varied before, during, and after the application of combined dc and ac magnetic fields for the six different electrolytes used. Except for 1 mM MgCl_2 , which seemed to be an unstable preparation, the ratio was generally higher during the applied fields than before. Also, the ratio was higher during the applied fields than after they were removed. This data seems to indicate that the applied magnetic fields affected the dc current through the membranes. Furthermore, in some cases, the ratio was higher for the post-field controls than for the pre-field controls, perhaps indicating that the application of the magnetic fields irreversibly affected the membranes in some way.

Some indications of how age might affect membrane response can be obtained by comparing Figs. 3.16 and 3.17. Since the average age of the post-field controls is generally greater than that of the membranes with fields applied, the greater instability of the membranes with the fields applied cannot be attributed solely to age. Another aspect of age of the membranes is shown in Fig. 3.18 which shows the active field runs as a function of membrane age. Active field runs are defined as those runs showing a response at least three standard deviations above the mean value. The data in Fig. 3.18 does not show any clear effect of age on membrane instability.

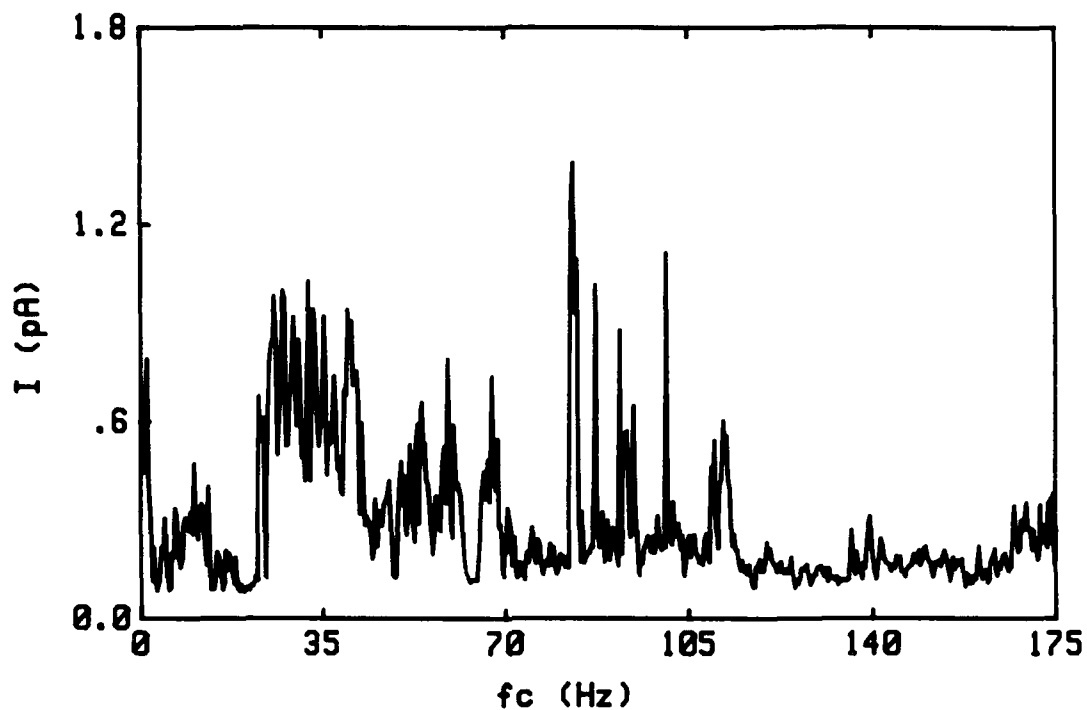


Figure 3.12 Field run showing dc current as a function of dc magnetic field strength calibrated in terms of the cyclotron frequency f_c (step size = 0.6 Hz). $f = 100$ Hz (frequency of ac fields), $f_{c1} = 100$ Hz (cyclotron frequency of ac magnetic field; $B_1 = 130 \mu\text{T}$). Electrolyte: 1 mM CaCl_2 . $V_{dc} = 60$ mV across the membrane. Standard deviation of the current is 0.213 pA. Ratio of the standard deviation to the mean is 0.723. Same membrane as in Fig. 3.10.

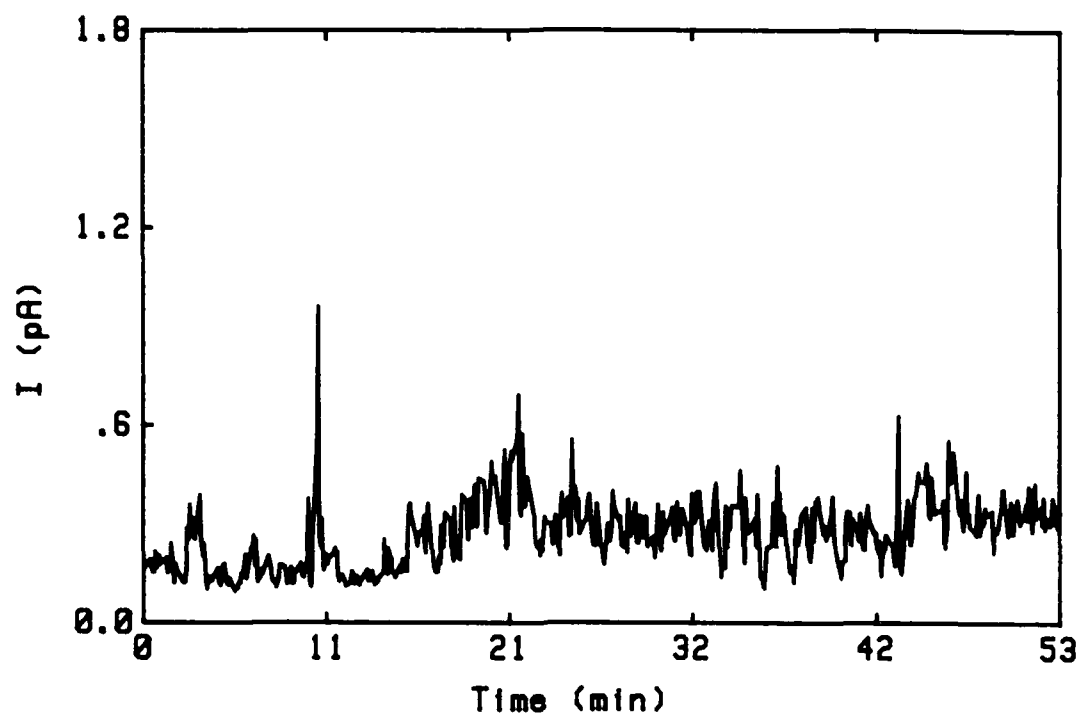


Figure 3.13. Control run showing dc current as a function of time. Electrolyte: 1 mM CaCl_2 . $V_{\text{dc}} = 60$ mV across the membrane. Standard deviation of the current is 0.105 pA. Ratio of the standard deviation to the mean is 0.387. Same membrane as in Fig. 3.10.

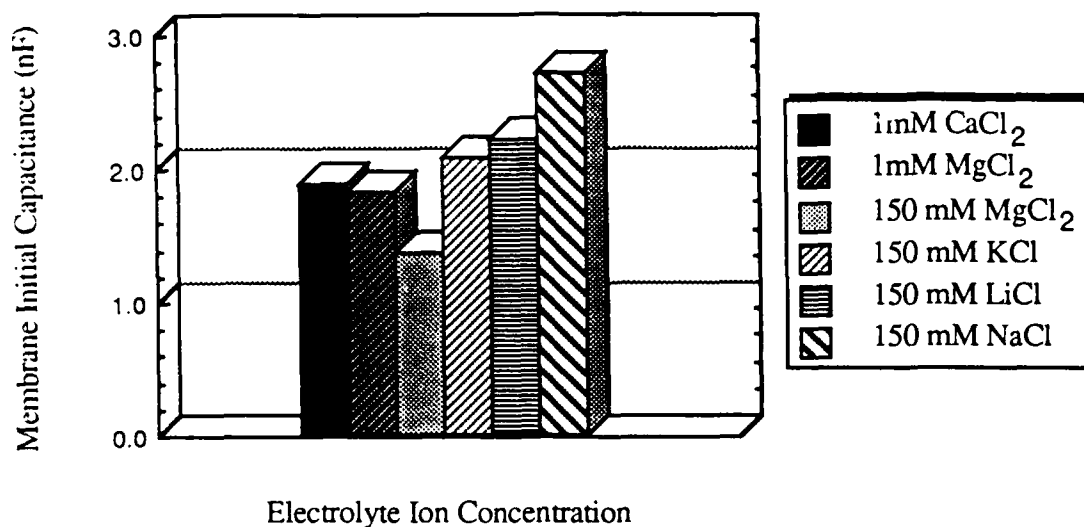


Figure 3.14. Initial membrane capacitance for the ions and concentrations used. These data were collected after the membrane had stabilized, typically during the the end of the first hour of forming the membrane and previous to turning off the ac triangle wave voltage that was used to measure membrane capacitance.

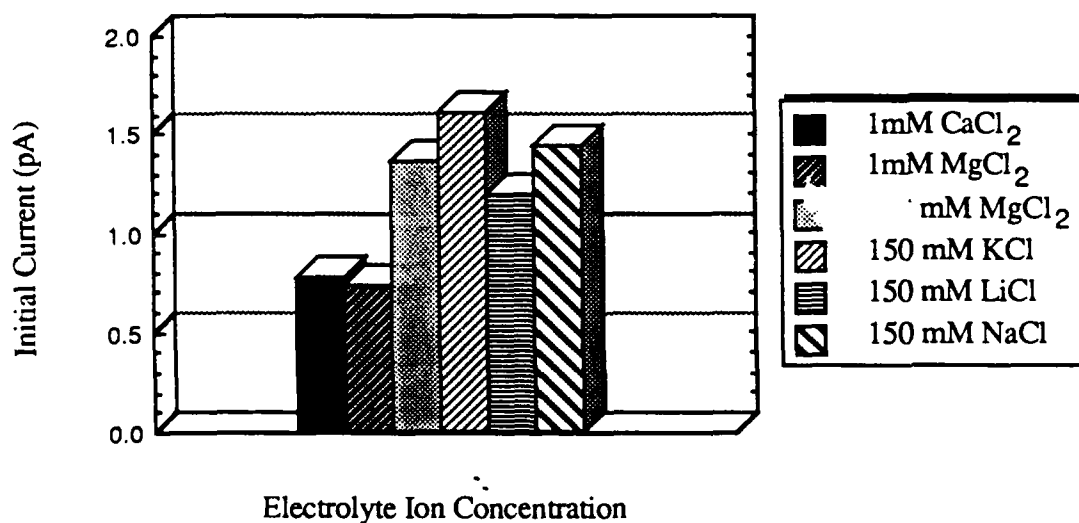


Figure 3.15 The mean value of initial dc current of each membrane for which the mean dc current was below 10 pA. Initial current is the value of current after the membrane had stabilized (typically one hour after formation), but before data was collected, either for controls or those exposed to magnetic fields.

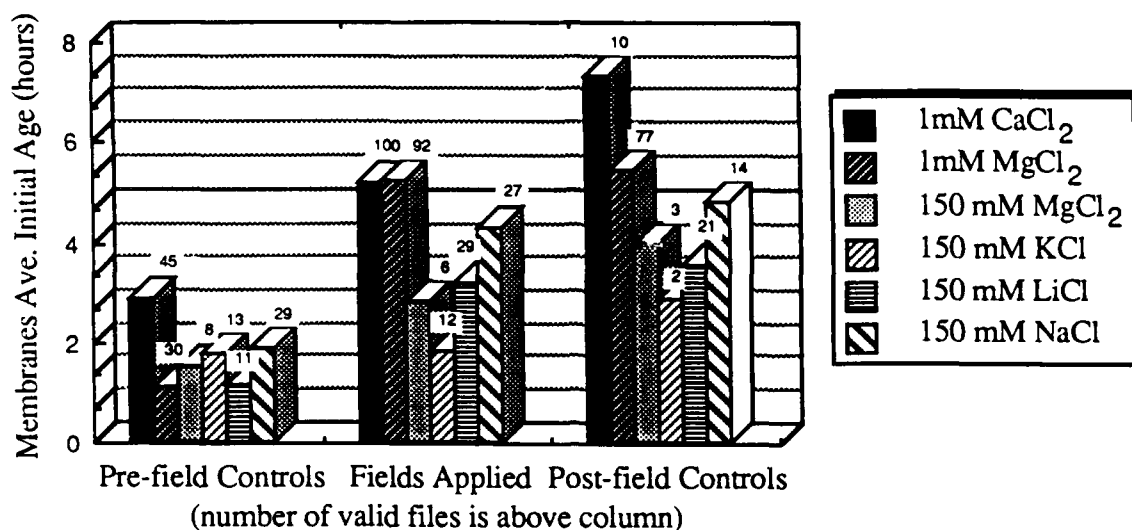


Figure 3.16. Average age of membranes as a function of applied magnetic fields for various electrolytes. Controls are membranes with no magnetic fields applied. Pre-field controls are those control runs having no field runs applied previously. Fields applied are those runs with fields applied. Post-field controls are control runs taken after fields had been applied to the membrane. The number of files (data runs) used is shown above the bar chart. More than one file was made for some membranes.

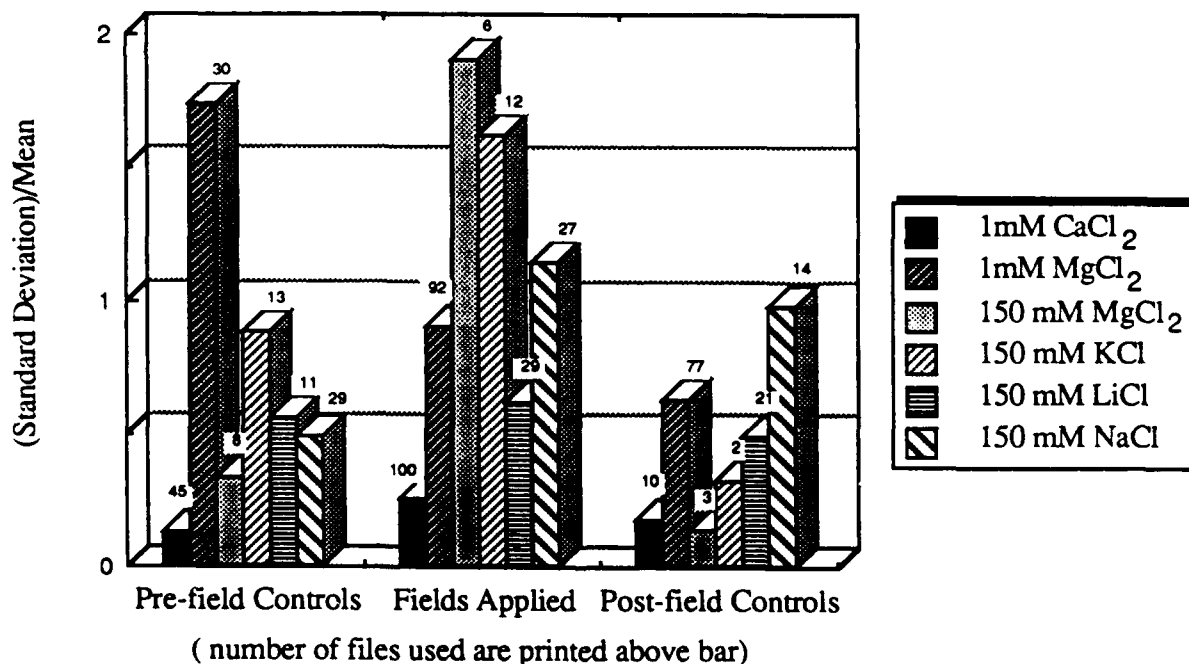


Fig. 3.17. Fluctuations in dc current before, during, and after exposure to combined dc and ac magnetic fields. Controls are membranes with no magnetic fields applied. Pre-field controls are those control runs having no field runs applied previously. Fields applied are those runs with fields applied. Post-field controls are control runs taken after fields had

been applied to the membrane. The number of files (data runs) used is shown above the bar chart.

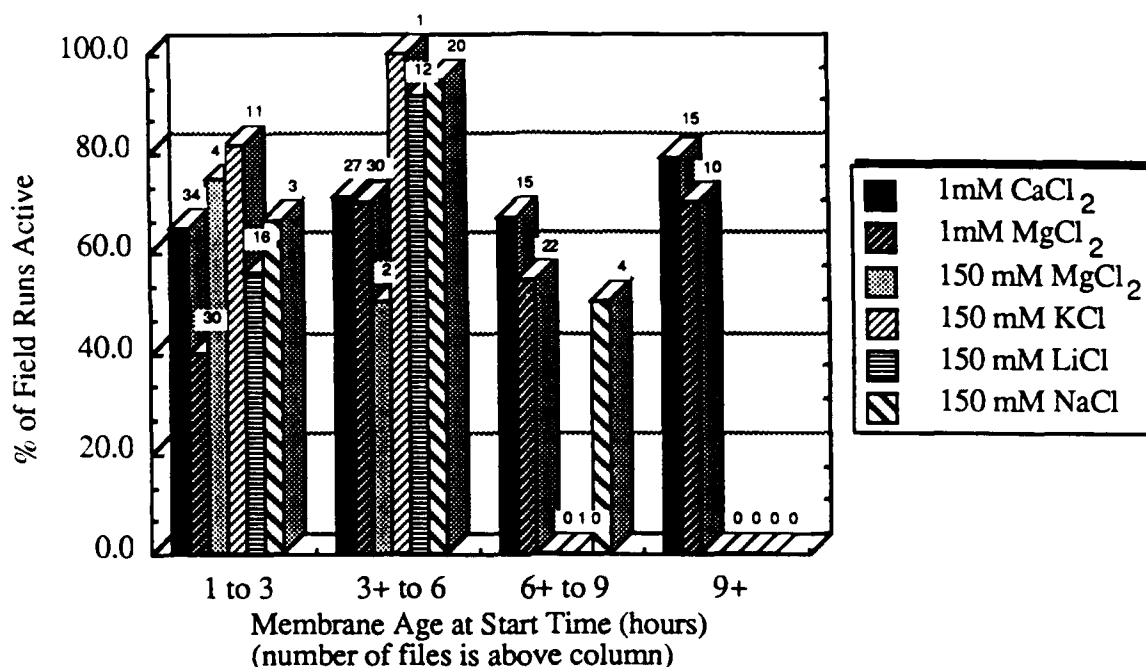


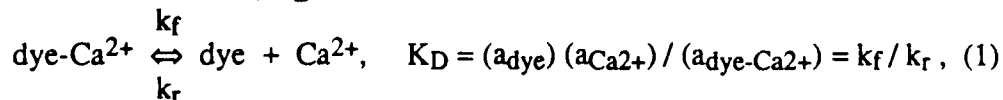
Figure 3.18. Fluctuations in dc current as a function of membrane age. Active field runs are defined as those runs showing a response at least three standard deviations above the mean value.

4.0 MEASUREMENTS OF CALCIUM BINDING TO METALLOCHROMIC DYES AND CALMODULIN

As we explained in Section 3.1, we investigated the possibility that the dc-ac magnetic fields affect calcium binding, but not in a membrane, by measuring whether dc-ac magnetic fields affect the complexing of metallochromic dyes with calcium and whether they affect the binding of calmodulin to calcium.

4.1 Murexide and Arsenazo III

Murexide and arsenazo III are metallochromic indicators: they change color upon complexation with calcium ions. These dyes are widely used in biology since they are insoluble in membranes and do not affect cell structure or function at the concentrations typically used for Ca²⁺ measurements. The dye and the dye-Ca²⁺ absorbance maxima for these two indicators differ enough to allow quantitative Ca²⁺ determination. The color of the solution depends on the ratio of free dye to calcium-bound dye. This equilibrium is described by the dissociation constant, K_D:



where k_f and k_r are the forward and reverse rate constants, and "a" refers to the activity of each compound. At low concentrations, the activities are equivalent to concentrations. For

the reaction mechanism shown above, the rate constants can be used to describe the rates of formation (concentration / time) of the species:

$$-d[\text{dye-Ca}^{2+}]/dt = d[\text{dye}]/dt = d[\text{Ca}^{2+}]/dt = k_f[\text{dye-Ca}^{2+}] - k_r[\text{dye}][\text{Ca}^{2+}]. \quad (2)$$

The goal of our experiments is to test whether or not low-frequency ac and dc magnetic fields affect the equilibrium or the absorbance shift due to the binding of Ca^{2+} to the dye. For example, if the applied magnetic fields decrease the affinity of Ca^{2+} for the dye, the equilibrium will shift to the right in reaction (1) and K_D will increase. Since the dissociation equilibrium can also be written as the ratio of the forward and reverse rate constants, as shown in equation (1), we can also think of an increase in K_D (or decrease in the Ca^{2+} -dye affinity) as an increase in the forward rate constant (k_f) relative to the reverse rate constant (k_r). Intuitively, it seems that it might be possible for the magnetic fields to affect k_f and k_r differently, since these rate constants differ by three orders of magnitude for murexide and about five orders of magnitude for arsenazo III (see Table 1). Our experiments did not investigate the reaction kinetics described in equation (2), so a proportional shift in k_f and k_r would not be detected by our equilibrium measurements.

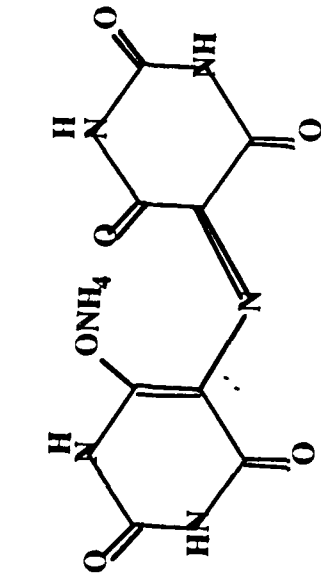
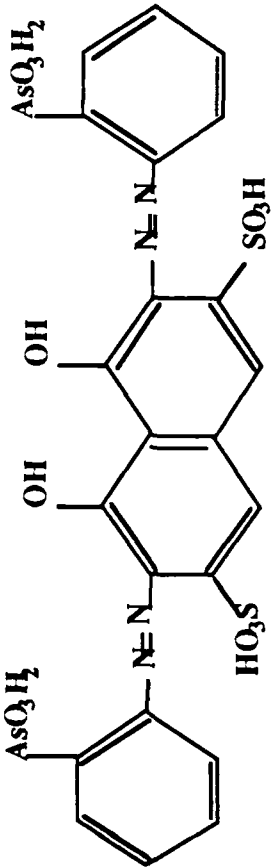
Table 1 shows the molecular structures and molecular weights of murexide and arsenazo III along with the dissociation constants found by Scarpa et al [1978]. The K_D for arsenazo is two orders of magnitude smaller than murexide, indicating that arsenazo binds Ca^{2+} much stronger than murexide binds Ca^{2+} . The dissociation constants as well as absorbance changes can vary several-fold depending on the experimental conditions, so most researchers produce [calcium ion concentration] vs. [absorbance] calibration curves for their particular conditions.

The wavelengths chosen for absorbance measurements depend on the turbidity of the solution, other cations present, and interfering absorbances of other materials present. In biological preparations which are turbid, a dual wavelength measurement is preferable to allow the measurement of the absorbance difference between a peak and an isobestic point (a wavelength at which the absorbance does not change with Ca^{2+}). The variations due to nonspecific absorption changes will be negligible if the reference wavelength lies only 5 to 40 nm from the measured wavelength [Scarpa et al, 1978].

The absorbance peaks for murexide and murexide- Ca^{2+} are at 540 and 470 nm with an isobestic point at 507 nm. Scarpa [1972] recommends the use of 540 and 507 because there is more nonspecific light scattering in biological solutions at 470 nm. Since our solutions were homogeneous, we chose to use 470 and 507 nm, which more than doubles our sensitivity for Ca^{2+} . We could have increased our sensitivity for Ca^{2+} even further by choosing 470 and 540 nm; however, these wavelengths are more than 40 nm apart, so nonspecific absorption affects (such as light source fluctuations) would more likely differ at these two wavelengths.

While murexide is selective for Ca^{2+} at the absorbance maxima, the arsenazo (561nm) and arsenazo- Ca^{2+} (595nm) peaks are affected by the presence of Mg^{2+} . The maximum absorbance of the arsenazo- Mg^{2+} complex occurs at 608 nm. Biological preparations typically contain Mg^{2+} , so the wavelengths chosen for Ca^{2+} detection are usually 675 and 685 nm [Scarpa et al, 1978]. Since our solutions do not contain Mg^{2+} , we chose to use 561 and 595 nm. These wavelengths maximize Ca^{2+} sensitivity and are within 40 nm of one another.

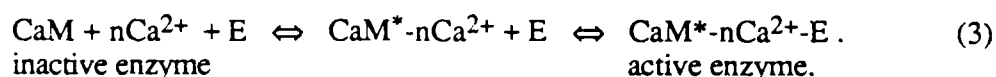
Table 1
The Properties of Murexide and Arsenazo III

MUREXIDE	ARSENAZO III
	
Ammonium purpurate	O-(1,8-Dihydroxy-3,6-disulfonaphthalene-2,7 bisazo)-bisbenzenearsonic acid
Molecular wt.	776
K _D from Scarpa et al, [1978] (at 50 mM and 0.5 M KCl)	15-60 μM

4.2 Calmodulin

A more interesting system is provided by calcium-calmodulin interactions. Since calmodulin that is complexed with calcium activates many enzymes, it provides a mechanism in which Ca^{2+} may affect different cellular functions of many organisms. Calmodulin is a small protein (molecular weight 16,790) which has been detected in eukariotic organisms ranging from plants to electric eels to bovine. In fact, calmodulin has been found in all eukariotic cells so far examined [Forsen et al, 1986]. This globular protein contains 148 amino acids, with a large content of acidic side chains (isoelectric point 3.9-4.3). Except for small differences, the amino acid composition is preserved from organism to organism, and contains no tryptophan and usually no cysteine.

In conjunction with Ca^{2+} , this protein stimulates the action of many enzymes by the following sequence of events:



When calmodulin binds calcium it undergoes a conformational change which includes a 5 to 10% increase in the α helix content of the protein. This $\text{CaM}^* \cdot n\text{Ca}^{2+}$ complex then binds to an enzyme to form an enzymatically active ternary complex. Enzymes which are known to be activated by calmodulin include: cyclic nucleotide phosphodiesterase, brain adenylate cyclase, ATPase and Ca^{2+} pumps of erythrocyte membranes, myosin light chain kinases, brain membrane kinases, phosphorylase b kinase, and NAD kinase. Calmodulin may also be involved in the assembly of microtubules, and by affecting protein kinase activities calmodulin will indirectly influence a wide variety of cellular processes [Klee et al, 1980].

Although there is some controversy regarding the affinities of the calcium binding sites, it is generally accepted that there are four Ca^{2+} binding sites which all have dissociation constants (K_D) in the micromolar range. Many researchers believe that the first two sites bind calcium cooperatively and with a higher affinity than the other two sites. Most of the conformational changes occur with the binding of the first two Ca^{2+} , but the more subtle changes which occur when the final two Ca^{2+} bind are often required for an active conformation [Hartshorne, 1985]. Klee et al [1983] postulate that these stepwise conformational changes may allow calmodulin to translate Ca^{2+} concentration changes into different cellular responses if different enzymes recognize different $\text{CaM} \cdot n\text{Ca}^{2+}$ conformations.

The color change of a dye/ Ca^{2+} solution can be used to measure the calmodulin/ Ca^{2+} equilibrium indirectly. The following two coupled equilibria must be considered for a solution containing dye, Ca^{2+} , and calmodulin:



Since the cooperativity and binding constants for the four Ca^{2+} binding to calmodulin are not known, we can not quantitatively predict the effect that equilibrium (5) will have on the dye- Ca^{2+} to dye ratio.

Qualitatively, since calmodulin binds Ca^{2+} three orders of magnitude stronger than murexide binds Ca^{2+} , we can assume that calmodulin will reduce the free Ca^{2+} concentration in murexide solutions by four times the calmodulin concentration (if each calmodulin binds four Ca^{2+}). But, since murexide relatively weakly binds to Ca^{2+} , the concentration of Ca^{2+} used for murexide experiments is very high--1 mM. So, a large addition of

calmodulin would be required to alter the murexide absorbance spectrum. Each absorbance sample must be at least 3 ml in volume (for our experimental set-up), so the total amount of calmodulin which would be necessary for murexide competition experiments is prohibitively expensive.

On the other hand, Ca^{2+} concentrations for arsenazo experiments are in the 5 to 10 μM range. Since the calmodulin binds Ca^{2+} about 1 order of magnitude stronger than arsenazo binds Ca^{2+} , approximately 1 μM additions of calmodulin should change the arsenazo absorbance spectrum.

4.3 Experimental Methods

The murexide solutions used for absorbance experiments contained 1 mM CaCl_2 and 0.1 mM murexide. The reagent grade CaCl_2 was obtained from Aldrich and the murexide was obtained from Sigma.

Arsenazo III absorbance experiments were done using 25 μM arsenazo III, 100 mM KCl, 10 mM HEPES (pH 7.5), and 5 μM CaCl_2 dissolved in deionized and doubly distilled water. The KCl (gold label), HEPES (gold label), and a sodium salt of arsenazo III (A-8891) were obtained from Sigma. The arsenazo III contained less than 0.2 mole fraction of Ca^{2+} , so the 25 μM arsenazo solution included less than 5 μM of Ca^{2+} contamination. The concentration of Ca^{2+} listed for the arsenazo solutions in this report is in addition to the Ca^{2+} contamination. Therefore, the 5 μM CaCl_2 solutions may contain as much as 10 μM Ca^{2+} .

For calmodulin experiments, the arsenazo solutions also contained 4 μM calmodulin. The calmodulin, derived from bovine brain, was more than 98% pure and obtained from Sigma (activity listed as 70,000 units/mg calmodulin). The moles of calmodulin added to solutions was determined by assuming that 98% by mass of the calmodulin consists of active (Ca^{2+} binding) protein.

4.3.1 Optics. The sample absorbance was measured using a Guided Wave Model 200-50 fiber optic spectrum analyzer. This instrument allows the measurement of the absorbance at a single wavelength at a time. The optrode tip, shown in Fig. 4.1, was immersed into the sample. The incident light from a tungsten/halogen lamp passed through the central fiber (320 μm diameter quartz core); and a rhodium mirror reflected light back into the 6 collection fibers surrounding the central fiber. The distance from the mirror to the distal end of the fibers was adjusted to about 3.5 mm, giving a path length of 7 mm.

As discussed in the introduction, the collection wavelengths chosen were 470 nm (λ_1) and 507 nm (λ_2) for murexide, and 561 nm (λ_1) and 595 nm (λ_2) for arsenazo. Consequently, the collection wavelength was scanned at 1 nm increments to include the appropriate wavelengths: 430-570 nm for murexide, and 520-620 nm for arsenazo. The two collection wavelengths were not measured at precisely the same time, but within the same scan time window. Five samples were averaged at each wavelength, so each scan took about 65 seconds for murexide and 45 seconds for arsenazo.

An IBM compatible personal computer along with Guided Wave software were used for spectrophotometer control as well as data storage. The Guided Wave software stores each absorbance scan in a separate ASCII file. An FT100 system was used to transfer the ASCII data files to MacIntosh floppy disks. Then, the data from each experiment was reformatted into a single file containing the following absorbance information as a function of time:

1. absorbance(λ_1)
2. absorbance(λ_2)
3. diff=absorbance(λ_1)-absorbance(λ_2)
4. normDiff= diff(time) - [diff(time+1)+diff(time-1)]/2 .

4.3.2 Magnetic Field Runs. In the following discussion the magnitudes of the ac and dc magnetic fields are expressed as the equivalent resonant frequency (Hz) with Ca^{2+} as the charged mass. A baseline for the absorbance of the solution was taken by applying no magnetic fields for the first 30-60 minutes (except the earth's vertical field was compensated). Then an ac magnetic field of magnitude f_{c1} and frequency f was applied to the system. The ac magnetic field waveform was either a sine or a square wave. The magnitude of the dc magnetic field was stepped from 0 to 230 Hz at about 1 Hz increments. Each dc field was applied for 90 (murexide) or 75 seconds (arsenazo) to allow collection of an absorbance scan. Before applying the next magnetic field combination, a control absorbance scan was collected while the earth's horizontal and vertical fields were compensated but no additional fields were applied. This alternation of field and control absorbance scans took about 11 1/2 hours for murexide and 9 1/2 hours for arsenazo.

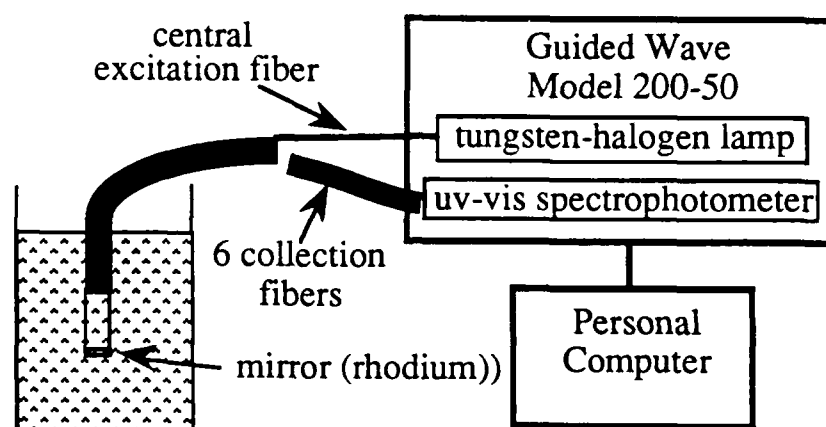


Fig. 4.1. A schematic of the experimental set-up for absorbance measurements. The fiber optic probe is immersed in the sample. The incident light from a tungsten-halogen lamp passes through the central fiber into the solution. A rhodium mirror reflects the light back into the 6 collection fibers which surround the excitation fiber. The collected light intensity is measured at a series of wavelengths. The spectrophotometer control and the data storage is managed with an IBM compatible personal computer.

The normalized difference (normDiff) was calculated at each field scan. If the absorbance exhibits a slow drift with time, the normalization will be close to zero. A peak in the normalized difference which is above or below zero indicates the occurrence of a reversible magnetic field effect.

4.4 Results and Discussion

4.4.1 Calibration Curves. Calibration curves for the absorbance difference of murexide and arsenazo solutions as a function of Ca^{2+} concentration are shown in Figures 4.2 and 4.3. The solutions were titrated with Ca^{2+} by adding aliquots of 50 mM CaCl_2 (murexide solutions) or 5 and 0.5 mM CaCl_2 (arsenazo solutions) to produce the desired concentrations. When more Ca^{2+} is added to the murexide solution, the absorbance difference (470-507 nm) becomes more positive until saturation is reached at about 5 mM Ca^{2+} .

The concentration used in our experiments, 1 mM Ca^{2+} , is at the higher end of the steepest region (most sensitive region) of the calibration curve.

The Ca^{2+} concentrations for the arsenazo dye calibration curve are on the order of 10 μM , rather than 1 mM. Recall that these calcium concentrations may all be shifted to include up to 5 μM of additional Ca^{2+} . Since the absorbance curve with no added Ca^{2+} was almost perfectly symmetrical (only a barely distinguishable shoulder), we believe the shift is less than 1 μM . In any case, as the added Ca^{2+} concentration increases, the absorbance difference (561-595 nm) decreases until saturation is reached at about 40 μM . For our experiments we used 5 μM added Ca^{2+} , which lies within the most sensitive region of the calibration curve.

The calmodulin calibration curve is shown below in Figure 4.4. First, the absorbance difference of an arsenazo solution with no added Ca^{2+} was measured to be about 0.285. Then, a small amount of 0.5 mM CaCl_2 was injected into the sample. The resultant 5 μM solution of Ca^{2+} had a lower absorbance near 0.15. When 2 μM additions of calmodulin were made, the absorbance increased since the calmodulin was now binding some of the calcium previously bound to arsenazo. We chose to use 4 μM calmodulin solutions for subsequent calmodulin field runs.

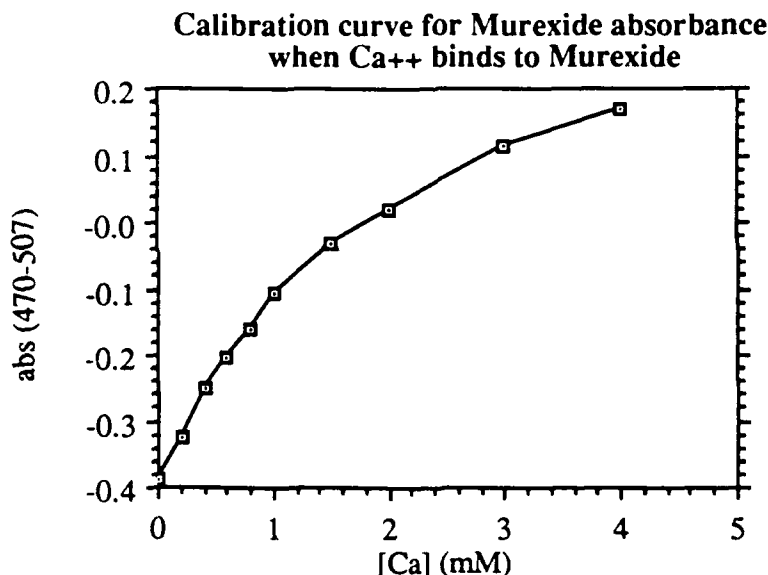


Figure 4.2. The absorbance difference (470-507 nm) of a solution containing 0.1 mM murexide increases as Ca^{2+} (as CaCl_2) is added to the sample. The murexide calibration curve is approximately linear when the Ca^{2+} concentration is less than 1 mM.

4.4.2 Murexide Experiments. The results of the eight murexide experiments are summarized in Table 2. Field runs were done with the ac magnetic field frequency set at 50 or 100 Hz. In addition to the sine waveforms, two experiments were done with a 50 Hz square wave. The magnitude of the ac field was $f_{c1}=50$ Hz, $f_{c1}=90$ Hz, $f_{c1}=100$ Hz, or $f_{c1}=120$ Hz. The noise level for each experiment was estimated to be the scatter of the normalized data from zero. The noise level ranged from ± 0.001 to ± 0.01 absorbance units. Since the magnitude of the measured absorbance difference is less than 0.5, this noise level is only 0.5 to 5% of the maximum difference. The noisiest experiment, ± 0.01 , would correspond to a 0.96 mM to 1.08 mM concentration deviation from 1 mM Ca^{2+} . This means

that a detectable magnetic field effect would have to alter the Ca^{2+} -murexide interaction more than a 4 to 8% change in Ca^{2+} concentration.

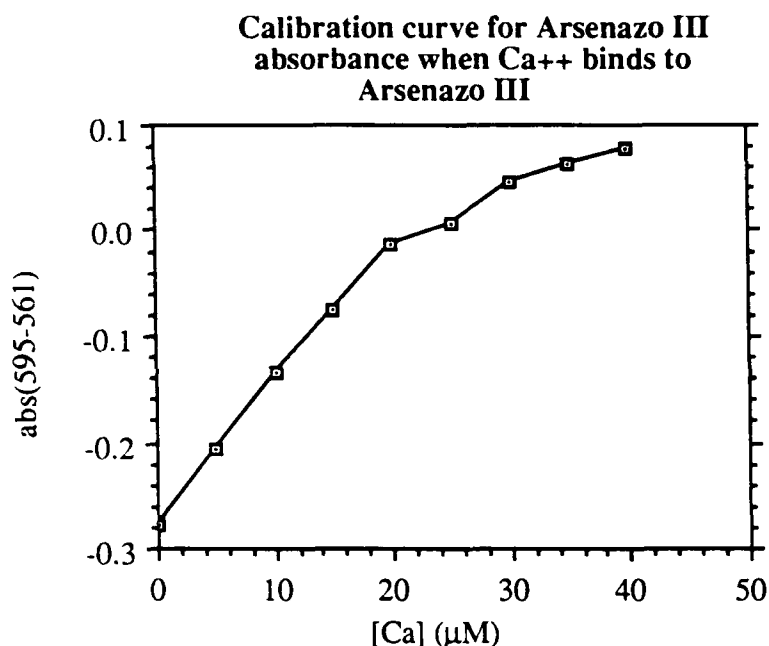


Figure 4.3. The arsenazo III calibration curve shows that the absorbance difference (595-561 nm) increases as Ca^{2+} is added to a solution containing 25 μM arsenazo III, 100 mM KCl, and 10 mM HEPES at pH 7.5. The absorbance difference is the most sensitive to Ca^{2+} addition when the Ca^{2+} concentration is less than 20 μM .

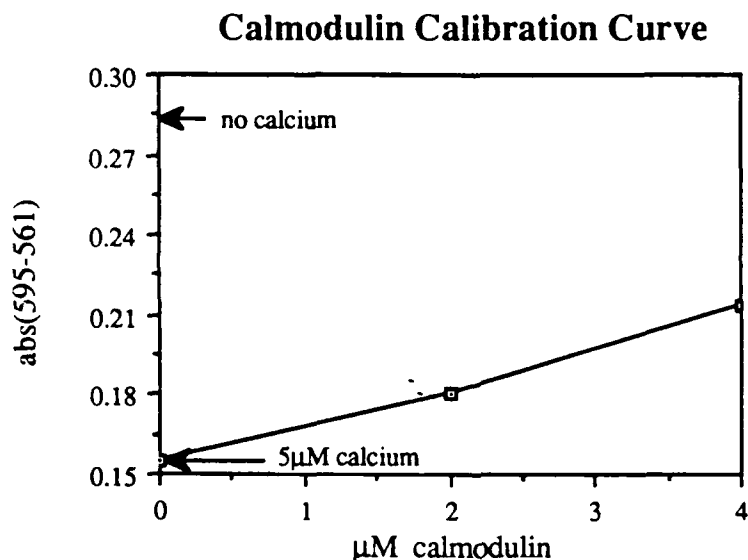


Figure 4.4. A solution containing 25 μM Arsenazo III, 100 mM KCl, 10 mM HEPES (pH 7.5), and 5 μM CaCl_2 was titrated with 2 μM aliquots of calmodulin. Due to the complexation of calmodulin with Ca^{2+} , when calmodulin is added the absorbance difference between 595 and 561 nm approaches the absorbance difference when no Ca^{2+} is in the solution.

4.4.3 Arsenazo Experiments. The complications created by the interaction of dye with the optrode (or material adsorbed on the optrode) as seen in experiment M0407, were a continual problem in the arsenazo experiments. The five field runs (3 with calmodulin) and six control runs using arsenazo are summarized in Table 3. In all experiments with the optrode immersed in the solution the absorbance drift was significant, ranging from 0.14 to 0.48. Even after cleaning the metal tip by sonicating in a soap solution and rinsing with copious amounts of methanol and doubly distilled deionized water, the absorbance changed significantly with time (0.29 for experiment A0409). This suggests that the arsenazo dye solution interacts with the metal optrode which consists of a stainless steel housing and rhodium mirror. The absorbance drift was not in one direction with time, and often included absorbance oscillations of 0.03 to 0.08 in magnitude with periods of 15 to 20 minutes.

Although no peaks were apparent above the normalized noise, the maximum values of occasional data points which are greater than the typical noise level are also listed in Table 2. The largest spikes were only three times the noise level. There were no apparent correlations between the spike frequency or location and the applied magnetic fields.

Since an absorbance experiment takes many hours, we expected the absorbance difference to drift with time due to photobleaching, solution evaporation, and temperature changes. The absorbance drift, however, was less than 0.07 in all experiments except one (M0407). The absorbance difference changed 0.37 in experiment M0407, which was conducted several months later than the rest of the experiments. We later discovered that the optrode had been immersed in protein (BSA and IgG) solutions in the interim, which may have adsorbed very strongly to the probe. The complex interactions between the adsorbed protein on the optrode, Ca^{2+} , and murexide in experiment M0407 were also not affected by the magnetic fields ($f=50$ Hz square, $f_{c1}=100$ Hz).

Arsenazo dye, and not the salt in the solution, appeared to be responsible for the drift. An experiment with 25 μM arsenazo (A0412) fluctuated 0.3 absorbance units in only 13 minutes; however, a salt control with no dye (A0410) did not measurably vary in 90 minutes. In addition, two absorbance experiments were done without the optrode immersed in the solution. Figure 4.5 shows that the absorbance at 595 nm as a function of time measured using a split beam Perkin Elmer Lambda 7 spectrophotometer does not change drastically with time. The light source was a tungsten/halogen lamp and a salt solution containing no dye was used as the reference. The split beam set up would decrease drifts which would affect both the sample and reference solutions, such as temperature. Over 600 minutes the drift was only 0.022 absorbance units and the noise was ± 0.002 . The drift was not linear, but formed a smooth curve and the drift was only 2% of the measured absorbance of about 1 (the path length was 10 mm).

Another experiment (A0417) was done with the fiber bundle above the level of the solution and a mirror under the vial to reflect the light back into the collection fibers. A rubber stopper was drilled to fit snugly around the optrode and into the vial to decrease solution evaporation. This experiment was done on a lab bench, while all of the other experiments were done on a vibration isolation table. As shown in Figure 4.6, during 140 minutes the drift was only 0.03 units of absorbance difference. In contrast, the absorbance fluctuations for the eight arsenazo experiments done with the optrode immersed in the solution ranged from 0.07 to 0.2 after 140 minutes. This also indicates that the large absorbance oscillations are caused by the immersion of the optrode into the solution.

The noise levels of the Guided Wave absorbance measurements of arsenazo solutions with the optrode immersed in solution ranged from ± 0.001 to ± 0.004 , which are

comparable to the absorbance uncertainty of the dual beam spectrophotometer (± 0.002). For the worst case (± 0.004) this uncertainty corresponds to a $\pm 0.31 \mu\text{M}$ Ca^{2+} concentration change ($\pm 6.2\%$ for a $5 \mu\text{M}$ solution). The absorbance noise for experiment A0417 with the optrode above the solution is greater at ± 0.006 (see Figure 4.6), which corresponds to a $0.46 \mu\text{M}$ or 9.2% Ca^{2+} concentration change. So, while eliminating the interactions caused by the optrode tip in the solution, positioning the fiber out of the solution

Table 2
Summary of the Murexide Experiments

Experiment	AC magnetic field	Noise level	Noise spikes	Signal drift	Experiment time (min)
M0203	$f = 50 \text{ Hz}$, square $fc1 = 100 \text{ Hz}$	± 0.01	± 0.02	0.01	900
M0407	$f = 50 \text{ Hz}$, square $fc1 = 100 \text{ Hz}$	± 0.0015	± 0.004	0.37	750
M0204	$f = 100 \text{ Hz}$, sine $fc1 = 50 \text{ Hz}$	± 0.005	± 0.01	0.01	900
M0202	$f = 100 \text{ Hz}$, sine $fc1 = 50 \text{ Hz}$	± 0.01	± 0.015	0.01	750
M1024	$f = 100 \text{ Hz}$, sine $fc1 = 90 \text{ Hz}$	± 0.002	± 0.006	0.07	700
M1021	$f = 100 \text{ Hz}$, sine $fc1 = 100 \text{ Hz}$	± 0.003	± 0.006	0.004	900
M1020	$f = 100 \text{ Hz}$, sine $fc1 = 120 \text{ Hz}$	± 0.001	± 0.002	0.035	1050
M1025	$f = 100 \text{ Hz}$, sine $fc1 = 120 \text{ Hz}$	± 0.003	± 0.006	0.04	750

Table 2. A summary of the eight murexide experiments with applied magnetic fields is shown above. The dc magnetic field was stepped from 0 to 230 Hz with 1 Hz increments. Variations in the absorbance difference (between 470 nm and 507 nm) of each experiment were used to estimate the noise level, noise spikes, and experimental drift.

Table 3
Summary of Arsenazo III Experiments

Experiment	AC field/ conditions	Noise level	Noise spikes	Signal drift	Experiment time (min)
A0308	control	± 0.002	± 0.03	0.114	620
A0409	control after cleaning	± 0.001	± 0.0018	0.29	750
A0413	control double sample vol.	± 0.003	± 0.01	0.48	260
A0417	control fiber out of soln.	± 0.006	± 0.012	0.03	140
A0410	control salt, but no dye	$\pm 2 \times 10^{-5}$	$\pm 2 \times 10^{-5}$	---	90
A0412	control 25 μM Arsenazo	± 0.003	---	0.3	13
A0228	f = 50 Hz, square fc1 = 100 Hz	± 0.0034	± 0.008	0.21	900
A0307	f = 100 Hz, sine fc1 = 120 Hz	± 0.004	± 0.008	0.36	675
A0304 calmodulin	f = 50 Hz, square fc1 = 100 Hz	± 0.002	± 0.01	0.28	750
A0306 calmodulin	f = 100 Hz, sine fc1 = 50 Hz	± 0.002	± 0.006	0.33	750
A0305 calmodulin	f = 100 Hz, sine fc1 = 100 Hz	± 0.0015	± 0.014	0.12	590

Table 3. The arsenazo III experiments are summarized above. The control experiments, with only the vertical component of the earth's magnetic field compensated are labelled "control". Experiments with 4 μM calmodulin added are labelled "calmodulin". The noise level, noise spikes, and experimental drift are variations in the absorbance difference (595 nm-516 nm) and were estimated from the data graphs.

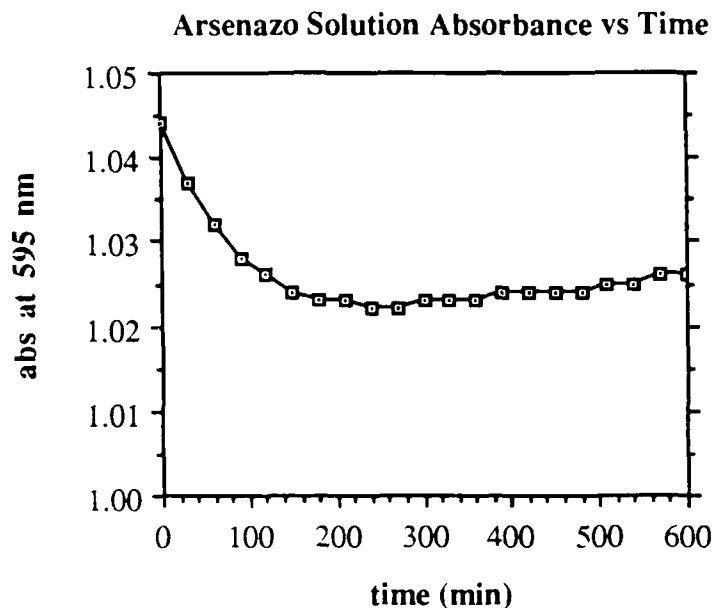


Figure 4.5. A split beam Perkin Elmer spectrophotometer was used to measure the absorbance (at 595 nm) versus time of an arsenazo solution containing 25 μM arsenazo III, 100 mM KCl, 10 mM HEPES (pH 7.5) and 5 mM CaCl_2 . The reference solution was the above salt solution without arsenazo. The absorbance drift over 10 hours is less than 0.025 absorbance units, and the absorbance noise is less than ± 0.002 .

increases the absorbance noise. This noise level might be decreased if the experiment is conducted on the vibration isolation table to decrease movement of the air/water interface.

The two arsenazo experiments done with applied magnetic fields (see Table 3) were not detectably different from the control runs. Although there were occasional normalized absorbance spikes, the frequency and magnitude of these spikes did not differ from the control runs. As with the control runs, the absorbance difference fluctuated significantly with time.

4.4.4 Calmodulin Experiments. The three field runs done with an addition of 4 μM calmodulin to the arsenazo solutions were not detectably different from the arsenazo control runs. The noise level for the calmodulin experiments ranged from 0.0014 to 0.01 absorbance units. Assuming the calmodulin calibration curve is linear near 4 μM calmodulin, this noise corresponds to a $\pm 0.67 \mu\text{M}$ change in calmodulin concentration. This means that a measurable field effect must at least be equivalent to a $\pm 16\%$ change in calmodulin. So, we can conclude that the magnetic fields do not measurably influence the complex processes occurring between the Ca^{2+} , arsenazo, calmodulin, and the optrode tip. Further experiments should be done with the fiber out of the solution to isolate the Ca^{2+} -arsenazo (and calmodulin) interactions and determine if the magnetic fields affect this interaction alone.

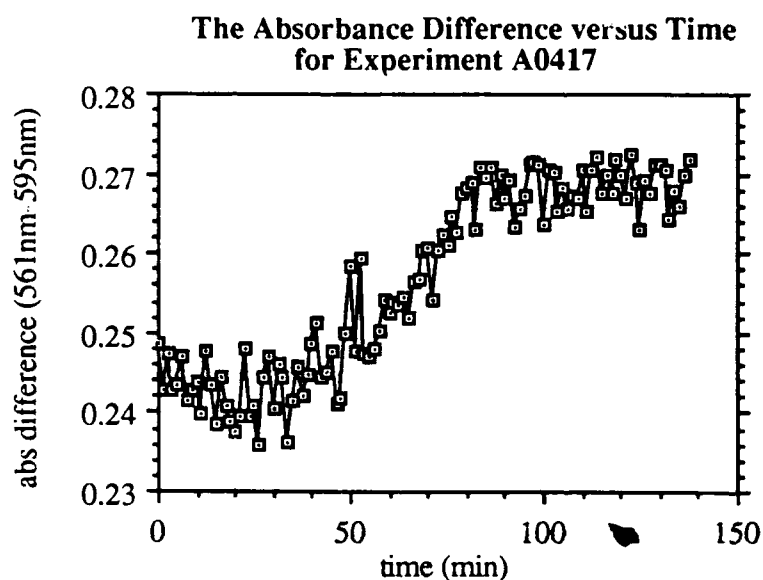
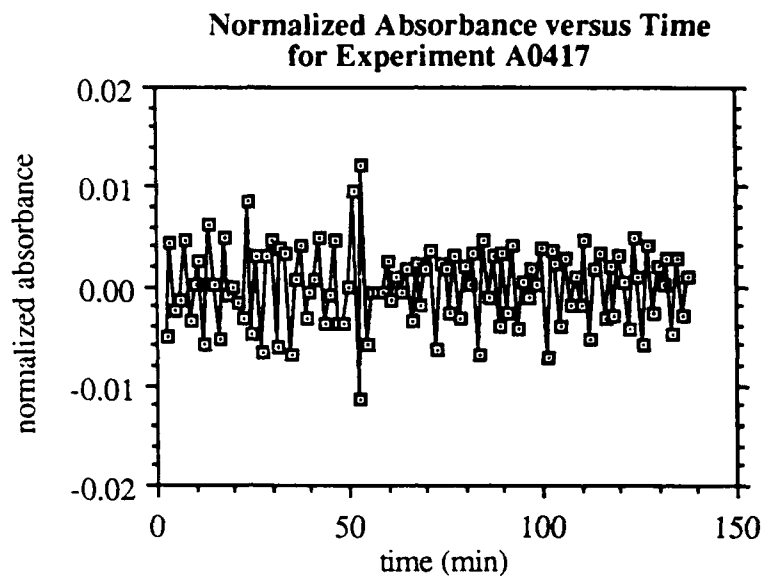


Figure 4.6. The results for the arsenazo control experiment (no applied fields) shown above were collected with the optical fiber above the solution. A mirror under the solution vial reflected light back into the collection fibers. The noise level and noise spikes for this experiment were estimated from graph (a) to be ± 0.006 and ± 0.012 , respectively. These values are larger than for experiments with the fiber optic probe immersed in the sample. The signal drift was estimated from graph (b) to be 0.03 absorbance units, which is 5 to 10 times less than typical experiments with the optrode immersed in the solution.

5.0 CONCLUSIONS

5.1 Membrane Studies

Our calculations of the effects of combined dc and ac magnetic fields on one charged particle in a viscous medium have given insight and for the first time have provided a physical basis for both frequency and amplitude windows. Furthermore, the calculated results make it clear that cyclotron-like resonance is very unlikely unless the responding charges experience very little viscous damping, or in other words, the collision frequency of the particles with their surroundings is of the same order of magnitude as the frequency of the applied ac fields.

Our measurements of the effects of combined dc and ac magnetic fields on planar phospholipid membranes have shown that the magnetic fields do affect the dc current through the membranes, but not in every membrane, and not consistently in any one membrane. Although the magnetic fields appeared to cause changes in dc current of several hundred percent, the changes did not occur at consistent magnetic field strengths, and they did not occur for conditions of cyclotron resonance of any of the ions that we tried. The experimental evidence rather points to some effect of the magnetic fields on the membranes themselves, not on the ion in the electrolyte. Since small vibrations of the membrane are known to have large effects on the dc current through it, one possible explanation of the magnetic field effects is that the magnetic fields excite resonant acoustic modes in the membrane, and these vibrations affect the dc current. An acoustic interaction is plausible because the membranes are about 1 mm in diameter and about 50 nm thick, which makes them very thin compared to diameter and therefore susceptible to mechanical vibrations.

5.2 Dye and Calmodulin Binding Experiments

In our experiments, the murexide- Ca^{2+} , arsenazo- Ca^{2+} , and calmodulin- Ca^{2+} equilibria were not measurably influenced by the application of ac and dc magnetic fields. Only a limited combination of fields, however, were applied to these systems, so it is possible that we have missed the resonant field combination(s) required for a response. In addition, it is possible that the field effect is too small to be detected by these experiments. Qualitatively, it is helpful to consider the calcium or calmodulin concentration changes that would be required to overcome the maximum absorbance noise observed for the three systems:

1. murexide-- a -4% to +8% change from 1 mM Ca^{2+} ,
2. arsenazo-- a $\pm 6.2\%$ change from 5 μM Ca^{2+} ,
3. calmodulin-- a $\pm 16\%$ change from 4 μM calmodulin.

Since the metal-containing fiber optic probe was immersed into the samples, the arsenazo and calmodulin experiments included arsenazo-optrode interactions as well as the desired arsenazo- Ca^{2+} interaction. So, it is possible that a field effect on the arsenazo- Ca^{2+} equilibrium was overwhelmed by the arsenazo-optrode interaction. Future work should include decreasing the absorbance uncertainty with the fiber optic probe out of the sample solution, so that the influence of the metal optrode housing or contamination on the optrode can be eliminated from the system.

5.3 General

None of our experiments have provided evidence that would support the cyclotron-resonance hypothesis of Liboff [McLeod and Liboff, 1986]. The experimental observations of Liboff and his colleagues indicate that the ion, particularly calcium, is responding as though it were bare, that is not solvated. Our calculations based on an elementary physical model indicate that cyclotron-like resonance would be very unlikely unless the collision frequency of the responding charged particles with their surroundings is of the

same order of magnitude as the ac frequency of the applied fields. These two facts taken together indicate that if cyclotron-like resonance is occurring in biological systems, it must occur in very special circumstances, since the ions are almost always solvated and almost never bare, and since the collision frequency with the surroundings is normally many orders of magnitude higher than the very low frequencies used in the experiments. Although an ion passing through a channel in a membrane could be unsolvated while in the channel, the transit time through the channel is so small compared to the period of the ac fields in the experiments that no resonance could occur while the ion is in the channel.

We conclude that the cyclotron-like resonant response observed by Liboff and his colleagues is presently unexplained, and more experimental evidence is needed to point to the site of the interaction. Experiments to search out the basic mechanism involved should certainly be done, as this phenomenon is one of the more robust and intriguing bioelectromagnetic effects ever observed.

REFERENCES

- Ashcroft, R.G., Coster, H.G. L., and Smith, J.R. "The Molecular Organization of Biomolecular Lipid Membranes." *Biochimica et Biophysica Acta*. 643:191-204 (1981).
- Bawin, S.M. and Adey, W.R. "Sensitivity of Calcium Binding in Cerebral Tissue to Weak Environmental Electric Fields Oscillating at Low Frequency." *Proc. Natl. Acad. Sci. USA* 72 (6):1999-2003 (1976).
- Blackman, C.F., Benane, S.G., House, D.E., and Joines, W.T. "A Role for the Magnetic Field in the Radiation-Induced Efflux of Calcium Ions from Brain Tissue In Vitro." *Bioelectromag.* 6:327-337 (1985).
- Blackman, C.F., Benane, S.G., Kinney, L.S., Joines, W.T., and House, D.E. "Effects of ELF Fields on Calcium-Ion Efflux from Brain Tissue In Vitro." *Radiation Research* 92:510-520 (1982).
- Cantor, C.S., Schimmel, P.R. *Biophysical Chemistry*. Volumes I and III, Chapters 4, 5, and 25, San Francisco: W.H. Freeman and Company (1980).
- Cevc, G., Marsh, D. *Phospholipid Bilayers, Physical Principles and Models*. Chapter 6, New York: John Wiley and Sons (1987).
- Chiabrera A., Bianco B., Caratozzolo F., Giannetti G., Grattarola M., Viviani R. "Electric and Magnetic Field Effects on Ligand Binding to the Cell Membrane." In Chiabrera A., Nicolini C., Schwan H.P. (eds): "Interactions Between Electromagnetic Fields and Cells." New York and London: Plenum (1985).
- Conti P., Gigante G.E., Alesse E., Cifone M.G., Fieschi C., Reale M., Angeletti P.U. "A Role for Ca^{2+} in the Effect of Very Low Frequency Electromagnetic Field on the Blastogenesis of Human Lymphocytes." *Federation of European Biochemical Societies Letters* 181:28-32 (1985).
- Conti P., Gigante G.E., Cifone M.G., Alesse E., Ianni G., Reale M., Angeletti P.U. "Reduced Mitogenic Stimulation of Human Lymphocytes by Extremely Low Frequency Electromagnetic Fields." *Federation of European Biochemical Societies Letters* 162:156-160 (1983).
- Delgado, J.R., Leal, J., Monteagudo, J., and Gracia, M.G. "Embryological Changes Induced by Weak, Extremely Low Frequency Electromagnetic Fields." *J. Anatomy* 134(3): 533-551 (1982).
- Devaux, P and McConnell, H.M. "Lateral Diffusion in Spin-Labeled Phosphatidylcholine Multilayers." *J. Amer. Chem. Soc.* 94:4475 (1972).
- Durney, C.H., Rushforth, C.K. and Anderson, A.A. "Resonant ac-dc Magnetic Fields: Calculated Response." *Bioelectromag.* 9:315-336 (1988).

- Edidin, M. "Rotational and Translational Diffusion in Membranes." *Ann. Rev. Biophys. Bioen.* 3:179-201 (1974).
- Forsen, S., Vogel, H. J., and Drakenberg, T. "Biophysical Studies of Calmodulin." in Calcium and Cell Function Vol. VI (Cheung, W.Y. ed.), Academic Press, New York, 113-157 (1986).
- Hanai, T., Haydon, D.A., and Taylor, J. "An Investigation by Electrical Methods of Lecithin-in-Hydrocarbon Films in Aqueous Solutions." *Proc. Roy. Soc. (London)*. A281:377 (1964).
- Hartshorne, David J. "Calmodulin: An Introduction to Biochemical Aspects." in Calmodulin Antagonists and Cellular Physiology (Hidaka, H., and D. J. Hartshorne, eds.), Academic Press, New York, 3-12 (1985).
- Henn, F.A., Decker, G.I., Greenwalt, J.W., and Thompson, T.E. "Properties of Lipid Bilayer Membranes Separating Two Aqueous Phases: Electron Microscope Studies." *J. Mol. Biol.* 24:51-58 (1967).
- Israelachvili, J. N. Intermolecular and Surface Forces, with Applications to Colloidal and Biological Systems. Chapter 8, London: Academic Press (1985).
- Jafary-Asl A.H., Solanki S.N., Aarholt E., Smith C.W. "Dielectric Measurements on Live Biological Materials." *J. Biological Physics* 11:15-22 (1983).
- Keithley Instruments. Low Level Measurements. Section 2, Cleveland: Keithley Instruments (1984).
- Klee, C. B., Crouch, T. H., and Richman, T.G. "Calmodulin." *Ann. Rev. Biochem.* 49: 489-515 (1980).
- Klee, Claude B. "Versatility of Calmodulin as a Cytosolic Regulator of Cellular Function." in Affinity Chromatography and Biological Recognition (Chaiken, I. M. et al, eds.), Academic Press, New York, 55-67 (1983).
- Liboff A.R. "Cyclotron Resonance in Membrane Transport." In Chiabrera A., Nicolini C., Schwan H.P. (eds): "Interactions Between Electromagnetic Fields and Cells." New York and London: Plenum (1985).
- Liboff, A.R., Rozek, R.J, Sherman, M.L., McCleod, B.R., and Smith, S.D. "Ca-45 Cyclotron Resonance in Human Lymphocytes." *J. Bioelect.* 6(1):13-22 (1987).
- McLeod B.R., Liboff A.R. "Dynamic Characteristics of Membrane Ions in Multifield Configurations of Low-Frequency Electromagnetic Radiation." *Bioelectromag.* 7:177-189 (1986).
- Miller, C. and Racker, E. "Fusion of Phospholipid Vesicles Reconstituted with Cytochrome-c Oxidase and Hydrophobic Protein." *J. Biol.* 26:321 (1976).
- Montal, M. and Mueller, P. "Formation of Bimolecular Membranes from Lipid Monolayers and a Study of Their Electrical Properties." *Proc. Nat. Acad. Scie. U.S.* 69:3561-66 (1972).
- Montgomery, D. Bruce. Solenoid Magnet Design. Chapter 8, Wiley-Interscience (1969).
- Mueller, P.J.O. and Rudin, D.E. "Translocators in Bimolecular Lipid Membranes: Their Role in Dissipative and Conservative Bioenergy Transductions." *Curr. Top. Bioenerg.* 3:157-249 (1969).
- Scarpa, A., Brinley, F. J., Tiffert, T., and Dubyak, G. R. "Metallochromic Indicators of Ionized Calcium." *Annals New York Academy of Sciences* 86-112 (1978).
- Scarpa, Antonio "Spectrophotometric Measurement of Calcium by Murexide." *Methods in Enzymology* 24: 343-351 (1972).
- Smith, S.D., McLeod, B.R., Liboff, A.R., and Cooksey, K. *Bioelectromag.* 8:215-227 (1987).
- Stryer, L. Biochemistry. Chapter 10, San Francisco: W.H. Freeman and Company (1975).
- Thomas, J.R., Schrot, J., and Liboff, A.R. "Low-Intensity Magnetic Fields Alter Operant Behavior in Rats." *Bioelectromag.* 7:349-357 (1986).
- Tien, H.T. Bilayer Lipid Membranes, Theory and Practice. Chapter 5, New York: Marcel Dekker, Inc. (1974).

Ubeda A., Leal J., Trillo M.A., Jiminez M.A., Delgado J.M.R. "Pulse Shape of Magnetic Fields Influences Chick Embryogenesis." J. Anatomy 137:513-536 (1983).
Webster, J.G., Editor. Medical Instrumentation Application and Design. Chapter 5, Boston: Houghton Mifflin Company (1978).